

A GENERALIZED SPECTRAL COLLOCATION METHOD WITH TUNABLE ACCURACY FOR VARIABLE-ORDER FRACTIONAL DIFFERENTIAL EQUATIONS*

FANHAI ZENG[†], ZHONGQIANG ZHANG[‡], AND GEORGE EM KARNIADAKIS[†]

Abstract. We generalize existing Jacobi–Gauss–Lobatto collocation methods for variable-order fractional differential equations using a singular approximation basis in terms of weighted Jacobi polynomials of the form $(1 \pm x)^\mu P_j^{a,b}(x)$, where $\mu > -1$. In order to derive the differentiation matrices of the variable-order fractional derivatives, we develop a three-term recurrence relation for both integrals and derivatives of these weighted Jacobi polynomials, hence extending the three-term recurrence relationship of Jacobi polynomials. The new spectral collocation method is applied to solve fractional ordinary and partial differential equations with endpoint singularities. We demonstrate that the singular basis enhances greatly the accuracy of the numerical solution by properly tuning the parameter μ , even for cases where we do not know explicitly the form of singularity in the solution at the boundaries.

Key words. singular basis, Jacobi polyfractonomials, Jacobi polynomials, differentiation matrices, space-fractional Burgers equation

AMS subject classifications. 26A33, 65M06, 65M12, 65M15, 35R11

DOI. 10.1137/141001299

1. Introduction. In this paper, we focus on the computation of the variable-order fractional integrals and derivatives of the *weighted* Jacobi polynomials. Using the weighted Jacobi polynomials with negative exponent as the basis functions, we develop Jacobi–Gauss–Lobatto (JGL) collocation methods to solve fractional differential equations (FDEs) of variable and constant orders when a singularity at an endpoint appears.

Numerical computation of the fractional integrals and derivatives is the key to understand fractional calculus and solve FDEs of increasing interest in many fields of science and engineering; see, e.g., [2, 10, 20, 21, 23, 27]. It is important to develop numerical methods for FDEs as the exact solutions to FDEs are difficult to obtain in real applications, due to the nonlocality and complexity of the fractional differential operators, especially for variable-order FDEs. Recently, finite difference methods have been widely used to approximate fractional differential operators and FDEs with constant orders; see, e.g., [3, 11, 12, 15, 18, 22, 24, 25, 30, 43]. Some of these methods have been extended to the variable-order FDEs; see, e.g., [1, 4, 5, 29, 32, 42, 45, 47].

Spectral methods have been also applied to FDEs when the exact solutions are smooth; see, e.g., [17, 26, 33, 35, 37, 38, 41, 46]. As in the traditional spectral methods for integer-order differential equations (see, e.g., [14, 28]), it is extremely important

*Submitted to the journal's Methods and Algorithms for Scientific Computing section December 23, 2014; accepted for publication (in revised form) August 26, 2015; published electronically November 12, 2015. This work was supported by the MURI/ARO on “Fractional PDEs for Conservation Laws and Beyond: Theory, Numerics and Applications (W911NF-15-1-0562)”, and also by NSF (DMS 1216437). The second author of this work was partially supported by a startup fund from WPI.

<http://www.siam.org/journals/sisc/37-6/100129.html>

[†]Division of Applied Mathematics, Brown University, Providence RI, 02912 (Fanhai.Zeng@brown.edu, george.karniadakis@brown.edu).

[‡]Department of Mathematical Sciences, Worcester Polytechnic Institute, Worcester, MA, 01609 (zzhang7@wpi.edu).

to choose appropriate approximation bases in the spectral methods for FDEs. When the solution is smooth enough, the classical Jacobi polynomials (typically Legendre or Chebyshev polynomials) can be used as an approximation basis and the computation of the fractional integrals and derivatives of these bases was investigated in some works; see, e.g., [16, 17, 37, 41]. Unlike for the classical spectral polynomials, Zayernouri and Karniadakis obtained a new basis in terms of polyfractonomials, which are eigenfunctions of the fractional Sturm–Liouville problem [36].

When the solutions of underlying FDEs are not smooth, some weighted Jacobi polynomials can be used to accommodate the weak singularity at the boundary; see, e.g., [6, 37, 38, 44]. Specifically, we use a set of *weighted* Jacobi polynomials of the form $\{(1+x)^\mu P_j^{a,b}(x)\}_{j \geq 0}$ or $\{(1-x)^\mu P_j^{a,b}(x)\}_{j \geq 0}$, where $P_j^{a,b}(x)$ ($x \in [-1, 1]$, $a, b > -1$) is the Jacobi polynomial and $\mu > -1$. In [6, 37, 38, 39, 44], the parameters b and μ (or a and μ) are chosen to be the same so that the left (or right) fractional derivatives of these weighted polynomials have simple expressions; see also Corollary 4.3 in this paper. In particular, the polyfractonomials of Zayernouri and Karniadakis have similar structure but with $\mu = b \geq 0$ or $\mu = a \geq 0$ (see [38, 39]), while we allow that $\mu > -1$ and μ is not required to be equal to a or b . Moreover, the proper choice of μ (especially negative μ) results in significant improvement in accuracy of numerical solutions as shown in section 5.

When $\mu = 0$, we may use the three-term recurrence formulas of the Jacobi polynomials to derive recurrence formulas for fractional integrals and derivatives of the Jacobi polynomials; see, e.g., [16, 40]. In this paper, we extend this approach to compute constant-order fractional integrals and variable-order fractional integrals of the weighted Jacobi polynomials for arbitrary $a, b, \mu > -1$. Subsequently, the left (or right) Riemann–Liouville and Caputo fractional derivatives of $(1+x)^\mu P_j^{a,b}(x)$ (or $(1-x)^\mu P_j^{a,b}(x)$) can be derived via the corresponding fractional integrals of these weighted bases. The advantage of recurrence formulas for the left (or right) fractional integral of weighted Jacobi polynomials is that they exhibit very good stability in the numerical simulations. Under some conditions, it can be proven that the recurrence formulas may degenerate into a three-term recurrence relation and thus define an orthogonal system; see, e.g., Corollary 4.3.

Compared to Galerkin spectral methods, spectral collocation methods are more flexible to deal with complicated problems, such as FDEs with variable coefficients, multiterm FDEs, and variable-order FDEs; see, e.g., [13, 38]. In this paper, we develop spectral collocation methods by using the aforementioned *weighted basis* that can capture the weak singularity at the boundary of the exact solution to FDEs with constant or/and variable orders *even if the regularity is unknown*.

In the implementation of spectral collocation methods, we have to compute fractional differentiation matrices, i.e., the fractional derivatives of the *weighted* Lagrange interpolants, which result from the Jacobi–Gauss- (JG-) type quadrature nodes; see, e.g., [31, 34, 38, 40]. With the derived variable-order fractional integrals and derivatives of the weighted Jacobi polynomials, we actually unify the results of existing approaches of computing fractional differentiation matrices; see, e.g., $\mu = 0$ in [31, 34, 40] and $\mu = b$ or $\mu = a$ in [13, 38, 39].

Further, we can choose some μ with $-1 < \mu < 0$ which can lead to better accuracy than the case of taking $\mu \geq 0$ when the regularity of the exact solutions to the FDEs is very low and even unknown. Note that the regularity is indeed low for the FDEs with variable orders and nonlinear FDEs; see Example 5.3. To the best of our knowledge, the case we propose corresponding to $-1 < \mu < 0$ is new and one of the distinguished features that makes our work different from the existing work.

In summary, we briefly list the main contributions of the present work.

- (1) Spectral collocation methods are developed to solve variable-order FDEs using a singular basis in terms of weighted Jacobi polynomials of the form $(1 \pm x)^\mu P_j^{a,b}(x)$, $\mu > -1$.
- (2) An efficient three-term recurrence formula to calculate the fractional integrals of the weighted Jacobi polynomials is developed, which leads to the differentiation matrices of the Riemann–Liouville and Caputo fractional derivatives.
- (3) By tuning the index $-1 < \mu < 0$, FDEs with endpoint singularity can be solved with higher accuracy by the proposed spectral collocation method.

The remainder of this paper is outlined as follows. The definitions of the fractional calculus are introduced in section 2 and the spectral collocation method for fractional ordinary differential equations (FODEs) is presented in section 3. In section 4, the new differentiation matrices are developed. The spectral collocation methods for FDEs applied to numerical experiments are presented in section 5, and the conclusion is included in the last section.

2. Definitions. In this section, we introduce the definitions of the fractional integrals and derivatives with variable orders and their related properties.

DEFINITION 2.1 (see [47]). *For a function $f(x)$, $x \in [x_L, x_R]$, the left fractional integral (or the left Riemann–Liouville integral) with order $\alpha(x) > 0$ is defined by*

$$(2.1) \quad {}_{RL}D_{x_L, x}^{-\alpha(x)} f(x) = D_{x_L, x}^{-\alpha(x)} f(x) = \frac{1}{\Gamma(\alpha(x))} \int_{x_L}^x (x-s)^{\alpha(x)-1} f(s) ds,$$

and the right fractional integral (or the right Riemann–Liouville integral) with order $\alpha(x)$ is defined as

$$(2.2) \quad {}_{RL}D_{x, x_R}^{-\alpha(x)} f(x) = D_{x, x_R}^{-\alpha(x)} f(x) = \frac{1}{\Gamma(\alpha(x))} \int_x^{x_R} (s-x)^{\alpha(x)-1} f(s) ds,$$

where $\Gamma(\cdot)$ is Euler's gamma function.

DEFINITION 2.2 (see [47]). *The left Riemann–Liouville fractional derivative with order $\alpha(x) > 0$, $x \in [x_L, x_R]$, of the given function $f(x)$, $x \in [x_L, x_R]$, is defined by*

$$(2.3) \quad {}_{RL}D_{x_L, x}^{\alpha(x)} f(x) = \frac{1}{\Gamma(n-\alpha(x))} \left[\frac{d^n}{d\xi^n} \int_{x_L}^{\xi} (\xi-s)^{n-\alpha(x)-1} f(s) ds \right]_{\xi=x}$$

and the right Riemann–Liouville fractional derivative is defined by

$$(2.4) \quad {}_{RL}D_{x, x_R}^{\alpha(x)} f(x) = \frac{(-1)^n}{\Gamma(n-\alpha(x))} \left[\frac{d^n}{d\xi^n} \int_{\xi}^{x_R} (s-\xi)^{n-\alpha(x)-1} f(s) ds \right]_{\xi=x},$$

where n is a positive integer and $n-1 < \alpha(x) < n$.

DEFINITION 2.3 (see [32, 47]). *The left and right Caputo fractional derivatives with order $\alpha(x) > 0$, $x \in [x_L, x_R]$, of the given function $f(x)$, $x \in [x_L, x_R]$, are defined as*

$$(2.5) \quad {}_C D_{x_L, x}^{\alpha(x)} f(x) = \frac{1}{\Gamma(n-\alpha(x))} \int_{x_L}^x (x-s)^{n-\alpha(x)-1} f^{(n)}(s) ds,$$

$$(2.6) \quad {}_C D_{x, x_R}^{\alpha(x)} f(x) = \frac{(-1)^n}{\Gamma(n-\alpha(x))} \int_x^{x_R} (s-x)^{n-\alpha(x)-1} f^{(n)}(s) ds,$$

where n is a positive integer and $n-1 < \alpha(x) < n$.

For $n - 1 < \alpha(x) < n$, $n \in \mathbb{N}$, $x \in [x_L, x_R]$, we have the following properties [47]:

$$(2.7) \quad \begin{aligned} {}_{RL}D_{x_L,x}^{\alpha(x)}f(x) &= {}_CD_{x_L,x}^{\alpha(x)}f(x) + \sum_{k=0}^{n-1} \frac{f^{(k)}(x_L)(x-x_L)^{k-\alpha(x)}}{\Gamma(k-\alpha(x)+1)}, \\ {}_{RL}D_{x,x_R}^{\alpha(x)}f(x) &= {}_CD_{x,x_R}^{\alpha(x)}f(x) + \sum_{k=0}^{n-1} \frac{(-1)^k f^{(k)}(x_R)(x_R-x)^{k-\alpha(x)}}{\Gamma(k-\alpha(x)+1)}. \end{aligned}$$

3. Spectral collocation method for FODEs. In this section, we present one of the main contributions of this work, i.e., we present the spectral collocation method to solve FODEs by applying the new differentiation matrices (see section 4). Our spectral collocation method is more flexible with better accuracy than the existing ones. We also clarify when the new spectral collocation methods obtains better results than existing versions.

Consider the following FODE

$$(3.1) \quad \begin{cases} {}_CD_{x_L,x}^{\alpha(x)}u(x) + C(x)u(x) = f(x), & x \in (x_L, x_R), 0 < \alpha(x) < 1, \\ u(x_L) = 0. \end{cases}$$

To approximate the solution of u , we use the following basis

$$X_N^\mu = \{v | v = (x-x_L)^\mu P_n(x), \quad P_n(x) \in \mathbb{P}_N, n = 0, 1, \dots, N\}, \quad \mu > -1,$$

where \mathbb{P}_N is a set of algebraic polynomials of order no more than N over the domain $[x_L, x_R]$. Our collocation method for (3.1) is then to find an interpolant $I_N^{\mu,a,b,+}u \in X_N^\mu$ such that

$$(3.2) \quad \left[{}_CD_{x_L,x}^{\alpha(x)}I_N^{\mu,a,b,+}u(x) \right]_{x=x_j} + C(x_j)u_j = f(x_j),$$

where $I_N^{\mu,a,b,+}u(x) = (x-x_L)^\mu I_N^{a,b}v = (x-x_L)^\mu \sum_{j=0}^N v_j l_j(x)$ and $v_j = (x_j-x_L)^{-\mu} u_j$. Here $I_N^{a,b}$ is the JGL interpolation operator associated with the collocation points $x_j = \frac{(x_R-x_L)\hat{x}_j+x_L+x_R}{2} \in [x_L, x_R]$, where \hat{x}_j ($0 \leq j \leq N$) are the roots of $(1-x^2)(P_N^{a,b}(x))'$, and $P_N^{a,b}(x)$ is the N th-order Jacobi polynomial defined by (4.2). The Lagrange interpolation basis function $l_j(x)$ is the j th corresponding interpolation polynomial, i.e., it has value 1 at x_j and value 0 at points x_i ($i \neq j$).

In its matrix form, (3.2) can be expressed as

$$(3.3) \quad \mathcal{A}(u_1, \dots, u_N)^T = (f(x_1), f(x_2), \dots, f(x_N))^T - \mathcal{B}v_0,$$

where $\mathcal{A} \in \mathbb{R}^{N \times N}$ that satisfies

$$(\mathcal{A})_{j-1,k-1} = ((x_R-x_L)/2)^{-\alpha(x_j)} (\mathcal{D}_L)_{j,k} + C(x_j)\delta_{j,k}, \quad j, k = 1, 2, \dots, N,$$

and \mathcal{D}_L is defined by (4.39), while $\mathcal{B} \in \mathbb{R}^{N \times 1}$ satisfies

$$(\mathcal{B})_{j-1} = ((x_R-x_L)/2)^{-\alpha(x_j)} (\mathcal{D}_L)_{j,0}, \quad j = 1, 2, \dots, N.$$

With (3.2), we actually solve the following equation

$$(3.4) \quad {}_CD_{x_L,x}^{\alpha(x)}((x-x_L)^\mu v(x)) + C(x)(x-x_L)^\mu v(x) = f(x),$$

which is equivalent to (3.1) with $u = (x - x_L)^\mu v$. As pointed out in [44], the regularity of v can be much higher than u and thus the polynomial interpolation of v in (3.2) is more accurate than the polynomial interpolation of u itself. For example, when $a = b = 0$ (see, e.g., [19]), we have

$$(3.5) \quad \begin{aligned} \|I_N^{\mu,0,0,+} u - u\|_{\omega^{0,0}} &= \|(x - x_L)^\mu (I_N^{0,0} v - v)\|_{\omega^{0,0}} = \|I_N^{0,0} v - v\|_{\omega^{0,2\mu}} \\ &\leq \|I_N^{0,0} v - v\|_{\omega^{-1,-1}} \leq CN^{-r} \|\partial_x^r v\|_{\omega^{r-1,r-1}}, \end{aligned}$$

where $\omega^{a,b}(x) = (1-x)^a(1+x)^b$ and we have supposed $v \in H^r(I)$, $I = (-1, 1)$, $\mu > -1/2$. If $u(x)$ has very low regularity at the endpoint, say $u(x) = (x - x_L)^{0.1}$, then $v = (x - x_L)^{-\mu+0.1}$, which has higher regularity than $u(x)$ when $-1 < \mu < 0$. For FODE (3.1) with smooth $f(x)$ and $C(x)$, this is true when α is small; see, e.g., [11] and Remark 3.1.

The choice of μ is extremely important in practice. Here we prefer to choose $\mu \leq 0$ that will lead to $v_0 = v(x_L) = \lim_{x \rightarrow x_L^+} (x - x_L)^{-\mu} u(x) = 0$ ($\mu < 0$) or $v_0 = v(x_L) = u(x_L)$ ($\mu = 0$) whenever $u(x)$ is bounded. For $\mu > 0$, we need to know $v_0 = \lim_{x \rightarrow x_L^+} (x - x_L)^{-\mu} u(x)$ that is unknown if the JGL spectral collocation method is applied to (3.1), while arbitrary assignment of v_0 may lead to unsatisfactory accuracy; see $\mathcal{B}v_0$ in the right-hand side of (4.31), where $v_0 = \lim_{x \rightarrow x_L^+} (x - x_L)^{-\mu} u(x)$ is possibly not equal to zero when $\mu > 0$. Moreover, the derivation of the differentiation matrix \mathcal{D}_L in (4.31) avoids using $(1+x_0)^{-\mu}$ for JGL points ($x_0 = -1$), which is meaningless when $\mu > 0$; see also the numerical results in Tables 3–4 in Example 5.1, where we also choose $\mu > 0$ and let $v_0 = 0$ in the numerical simulation for comparison.

Remark 3.1. Even for the simple FDE with variable order as (3.1), the regularity of its solution is much more complicated than in the case of the constant-order FDEs. For example, when $f(x) = 1$, $\alpha(x)$ is smooth, and $C(x) = \phi_0 = 0$, the exact solution to (3.1) is $u(x) = \frac{(x-x_L)^{\alpha(x)}}{\Gamma(1+\alpha(x))}$. For such a simple case, the regularity of $u(x)$ at $x = x_L$ is low when $\alpha(x)$ is small. In contrast, $v(x) = (x - x_L)^{-\mu} u(x) = \frac{(x-x_L)^{\alpha(x)-\mu}}{\Gamma(1+\alpha(x))}$ can be smoother than u when $-1 < \mu < 0$. Then we have more accurate numerical solutions of $v(x)$ and thus expect more accurate numerical solutions of $u(x)$. See numerical examples for details in section 5.

4. Derivation of the differentiation matrices. In this section, we first develop the recurrence formulas to calculate the fractional integrals of the weighted Jacobi polynomials $P_{\pm,j}^{a,b,\mu}(x)$, where $P_{\pm,j}^{a,b,\mu}(x)$ is defined by

$$(4.1) \quad P_{\pm,j}^{a,b,\mu}(x) = (1 \pm x)^\mu P_j^{a,b}(x), \quad \mu > -1, x \in [-1, 1].$$

Then we derive the fractional derivatives of $P_{\pm,j}^{a,b,\mu}(x)$ from the corresponding fractional integrals of $P_{\pm,j}^{a,b,\mu}(x)$, which leads to the desired differentiation matrices associated with these weighted polynomials by a simple matrix-matrix multiplication.

The Jacobi polynomials $\{P_j^{a,b}(x)\}$, $a, b > -1$, $x \in [-1, 1]$ are given by the following three-term recurrence relation (see, e.g., [28]),

$$(4.2) \quad \begin{aligned} P_0^{a,b}(x) &= 1, \quad P_1^{a,b}(x) = \frac{1}{2}(a+b+2)x + \frac{1}{2}(a-b), \\ P_{j+1}^{a,b}(x) &= (A_j x - B_j) P_j^{a,b}(x) - C_j P_{j-1}^{a,b}(x), \quad j \geq 1, \end{aligned}$$

where

$$(4.3) \quad \begin{aligned} A_j &= \frac{(2j+a+b+1)(2j+a+b+2)}{2(j+1)(j+a+b+1)}, \\ B_j &= \frac{(b^2-a^2)(2j+a+b+1)}{2(j+1)(j+a+b+1)(2j+a+b)}, \\ C_j &= \frac{(j+a)(j+b)(2j+a+b+2)}{(j+1)(j+a+b+1)(2j+a+b)}. \end{aligned}$$

Let $\omega^{a,b}(x) = (1-x)^a(1+x)^b$. Then, one has

$$(4.4) \quad \int_{-1}^1 P_m^{a,b}(x)P_n^{a,b}(x)\omega^{a,b}(x) dx = \delta_{mn}\gamma_n^{a,b},$$

where δ_{mn} is the Kronecker delta function and

$$(4.5) \quad \gamma_n^{a,b} = \frac{2^{a+b+1}\Gamma(n+a+1)\Gamma(n+b+1)}{(2n+a+b+1)n!\Gamma(n+a+b+1)}.$$

In this section, we also use the following notation:

$$(4.6) \quad G_{L,j}^{a,b,\alpha,\mu}(x) = D_{-1,x}^{-\alpha}P_{+,j}^{a,b,\mu}(x), \quad x \in [-1,1],$$

$$(4.7) \quad G_{R,j}^{a,b,\alpha,\mu}(x) = D_{x,1}^{-\alpha}P_{-,j}^{a,b,\mu}(x), \quad x \in [-1,1].$$

4.1. Fractional integrals of the weighted Jacobi polynomials. In this subsection, we develop a recurrence formula to calculate the $\alpha(x)$ th-order left (or right) fractional integral of $P_{+,j}^{a,b,\mu}(x)$ (or $P_{-,j}^{a,b,\mu}(x)$).

We can compute $G_{L,j}^{a,b,\alpha,\mu}(x)$ by the following recurrence relation.

THEOREM 4.1. *Let $a, b, \mu > -1$ and $\alpha(x) > 0$, $x \in [-1, 1]$. Then $G_j = G_{L,j}^{a,b,\alpha,\mu}(x)$ defined by (4.6) and $H_j = \alpha(x)G_{L,j}^{a,b,\alpha+1,\mu}(x)$ satisfy, for $j \geq 1$,*

$$(4.8) \quad G_{j+1} = (A_j x - B_j)G_j - C_j G_{j-1} - A_j H_j,$$

$$\begin{aligned} H_{j+1} &= -(A_j + B_j)H_j - C_j H_{j-1} \\ &\quad - (\mu + 1 + \alpha)A_j \left(\widehat{A}_j H_{j-1} + \widehat{B}_j H_j + \widehat{C}_j H_{j+1} \right) \end{aligned}$$

$$(4.9) \quad + (1+x)\alpha A_j \left(\widehat{A}_j G_{j-1} + \widehat{B}_j G_j + \widehat{C}_j G_{j+1} \right),$$

where

$$(4.10) \quad \widehat{A}_j = \frac{-2(j+a)(j+b)}{(j+a+b)(2j+a+b)(2j+a+b+1)},$$

$$(4.11) \quad \widehat{B}_j = \frac{2(a-b)}{(2j+a+b)(2j+a+b+2)},$$

$$(4.12) \quad \widehat{C}_j = \frac{2(j+a+b+1)}{(2j+a+b+1)(2j+a+b+2)}.$$

We can compute $G_{R,j}^{a,b,\alpha,\mu}(x)$ in a similar fashion.

THEOREM 4.2. *Let $a, b, \mu > -1$ and $\alpha(x) > 0$, $x \in [-1, 1]$. Then $G_j = G_{R,j}^{a,b,\alpha,\mu}(x)$ defined by (4.7) and $H_j = \alpha(x)G_{R,j}^{a,b,\alpha+1,\mu}(x)$ satisfy, for $j \geq 1$,*

$$(4.13) \quad G_{j+1} = (A_j x - B_j)G_j - C_j G_{j-1} + A_j H_j,$$

$$\begin{aligned} H_{j+1} = & (A_j - B_j)H_j - C_j H_{j-1} \\ & - (\mu + 1 + \alpha)A_j \left(\widehat{A}_j H_{j-1} + \widehat{B}_j H_j + \widehat{C}_j H_{j+1} \right) \end{aligned}$$

$$(4.14) \quad + (1 - x)\alpha A_j \left(\widehat{A}_j G_{j-1} + \widehat{B}_j G_j + \widehat{C}_j G_{j+1} \right),$$

where \widehat{A}_j , \widehat{B}_j , and \widehat{C}_j are defined by (4.10), (4.11), and (4.12), respectively.

Remark 4.1. When $\mu = 0$ and $j \geq 1$, we have (see, e.g., [16, 40]),

$$\begin{aligned} G_{L,j+1}^{a,b,\alpha,0} = & \frac{A_j x - B_j - \alpha(x)A_j \widehat{B}_j}{1 + \alpha(x)A_j \widehat{C}_j} G_{L,j}^{a,b,\alpha,0} - \frac{C_j + \alpha(x)A_j \widehat{A}_j}{1 + \alpha(x)A_j \widehat{C}_j} G_{L,j-1}^{a,b,\alpha,0} \\ (4.15) \quad & + \frac{A_j \left(\widehat{A}_j P_{j-1}^{a,b}(-1) + \widehat{B}_j P_j^{a,b}(-1) + \widehat{C}_j P_{j+1}^{a,b}(-1) \right)}{\Gamma(\alpha(x)) \left(1 + \alpha(x)A_j \widehat{C}_j \right)} (x + 1)^{\alpha(x)}, \end{aligned}$$

$$\begin{aligned} G_{R,j+1}^{a,b,\alpha,0} = & \frac{A_j x - B_j - \alpha(x)A_j \widehat{B}_j}{1 + \alpha(x)A_j \widehat{C}_j} G_{R,j}^{a,b,\alpha,0} - \frac{C_j + \alpha(x)A_j \widehat{A}_j}{1 + \alpha(x)A_j \widehat{C}_j} G_{R,j-1}^{a,b,\alpha,0} \\ (4.16) \quad & + \frac{A_j \left(\widehat{A}_j P_{j-1}^{a,b}(1) + \widehat{B}_j P_j^{a,b}(1) + \widehat{C}_j P_{j+1}^{a,b}(1) \right)}{\Gamma(\alpha(x)) \left(1 + \alpha(x)A_j \widehat{C}_j \right)} (1 - x)^{\alpha(x)}. \end{aligned}$$

For initial values $G_{L,j}^{a,b,\alpha,\mu}(j = 0, 1)$ and $G_{R,j}^{a,b,\alpha,\mu}(j = 0, 1)$, we can easily obtain

$$\begin{aligned} G_{L,0}^{a,b,\alpha,\mu} &= \frac{\Gamma(\mu + 1)}{\Gamma(\mu + 1 + \alpha(x))} (1 + x)^{\alpha(x)+\mu}, \\ G_{L,1}^{a,b,\alpha,\mu} &= \frac{(a + b + 2)\Gamma(\mu + 2)}{2\Gamma(\mu + 2 + \alpha(x))} (1 + x)^{\alpha(x)+\mu+1} - (b + 1)G_{L,0}^{a,b,\alpha,\mu}, \\ G_{R,0}^{a,b,\alpha,\mu} &= \frac{\Gamma(\mu + 1)}{\Gamma(\mu + 1 + \alpha(x))} (1 - x)^{\alpha(x)+\mu}, \\ G_{R,1}^{a,b,\alpha,\mu} &= -\frac{(a + b + 2)\Gamma(\mu + 2)}{2\Gamma(\mu + 2 + \alpha(x))} (1 - x)^{\alpha(x)+\mu+1} + (a + 1)G_{R,0}^{a,b,\alpha,\mu}. \end{aligned}$$

The initial values of H_j ($j = 0, 1$) in Theorem 4.1 (or Theorem 4.2) can be obtained from the relation $H_j = \alpha G_{L,j}^{a,b,\alpha+1,\mu}$ (or $H_j = \alpha G_{R,j}^{a,b,\alpha+1,\mu}$).

When $\mu = b$ in Theorem 4.1 or $\mu = a$ in Theorem 4.2, we have simpler expressions.

COROLLARY 4.3. *Suppose that $\alpha(x)$, $x \in (-1, 1)$, is a real-valued function, $a, b > -1$. Then*

$$\begin{aligned} (4.17) \quad {}_{RL}D_{-1,x}^{\alpha(x)} P_{+,j}^{a,b,b}(x) &= \frac{\Gamma(j + b + 1)}{\Gamma(j + b + 1 - \alpha(x))} (1 + x)^{b-\alpha(x)} P_j^{a+\alpha(x), b-\alpha(x)}(x), \\ {}_{RL}D_{x,1}^{\alpha(x)} P_{-,j}^{a,b,a}(x) &= \frac{\Gamma(j + a + 1)}{\Gamma(j + a + 1 - \alpha(x))} (1 - x)^{a-\alpha(x)} P_j^{a-\alpha(x), b+\alpha(x)}(x). \end{aligned}$$

Proof. Equation (4.17) with constant fractional order α can be found in [6, 37, 44], which also holds for the variable-order $\alpha(x)$. For any $\alpha(x)$, (4.17) can be proven by using the explicit form of Jacobi polynomials (e.g., see p. 71 in [28]), the proof of which is omitted here. \square

Next, we investigate the stability of the recurrence formulas (4.15) and (4.16). When $b = 0$, we can easily verify that $\widehat{A}_j P_{j-1}^{a,b}(-1) + \widehat{B}_j P_j^{a,b}(-1) + \widehat{C}_j P_{j+1}^{a,b}(-1) = 0$ by using (A.1) and (4.10)–(4.12). In such a case, (4.15) becomes a three-term recurrence formula and defines an orthogonal system with respect to the weight function $\omega^{a+\alpha,0}(x) = (1-x)^{a+\alpha}$ when $a+\alpha, -\alpha > -1$ and α is a constant. Hence, the recurrence formula (4.15) is stable for constant-order α when $a+\alpha, -\alpha > -1$. For each $x_0 \in [-1, 1]$ and $\alpha_0 = \alpha(x_0)$, we find that $\{G_{L,j}^{a,b,\alpha_0,0}(x)\}$ defines an orthogonal system with respect to the weight function $\omega^{a+\alpha_0,0}(x) = (1-x)^{a+\alpha_0}$, $x \in [-1, 1]$. Thus, (4.15) is stable for variable-order $\alpha(x)$ when $a+\alpha(x), -\alpha(x) > -1$. Similarly, (4.16) defines an orthogonal system when $a = 0$, α is a constant, and $b+\alpha, -\alpha > -1$, thus is stable for variable-order $\alpha(x)$ when $b+\alpha(x), -\alpha(x) > -1$.

In general cases, i.e., $b \neq 0$ or $a \neq 0$, it is difficult to prove that the three-term recurrence formula (4.8)–(4.9) or (4.13)–(4.14) could define an orthogonal system. Thus, we numerically show their performance in stability. Here we only consider (4.8)–(4.9), since the situation is very similar for (4.13)–(4.14).

We will test two approaches of computing $G_{L,j}^{a,b,\alpha,\mu}(x)$ in (4.6): the recurrence formula (4.8)–(4.9) and the direct computation using the Gauss quadrature rule given by

$$(4.18) \quad G_{L,j}^{a,b,\alpha,\mu}(x) = \frac{(x+1)^{\alpha(x)+\mu}}{2^{\alpha(x)+\mu}\Gamma(\alpha(x))} \int_{-1}^1 \omega^{\alpha(x)-1,\mu}(\hat{s}) P_j^{a,b}\left(\frac{(x+1)\hat{s}+x-1}{2}\right) d\hat{s},$$

where $\omega^{\alpha(x)-1,\mu}(\hat{s}) = (1-\hat{s})^{\alpha(x)-1}(1+\hat{s})^\mu$. So for any given $x \in [-1, 1]$, $G_{L,j}^{a,b,\alpha,\mu}(x)$ can be directly calculated by the following exact formula

$$(4.19) \quad G_{L,j}^{a,b,\alpha,\mu}(x) = \frac{1}{\Gamma(\alpha(x))} \left(\frac{x+1}{2}\right)^{\alpha(x)+\mu} \sum_{k=0}^{M_j} \omega_k P_j^{a,b}(s_k), \quad M_j \geq \lceil j/2 \rceil,$$

where $s_k = \frac{(x+1)\hat{s}_k+x-1}{2}$, $\{\hat{s}_k\}$ are the JGL quadrature points, i.e., $\{\hat{s}_k\}$ are the roots of $(1-\hat{s}^2)\partial_{\hat{s}} P_{M_j}^{\alpha(x)-1,\mu}(\hat{s})$, with the corresponding weights $\{\omega_k\}$. For simplicity, we can choose $M_j = \lceil N/2 \rceil + 2$ in (4.19) in the computation.

Now we are ready to test the computational performance of the recurrence formula (4.8)–(4.9) and the Gauss quadrature (4.19). The numerical solutions obtained by the recurrence formula (4.8)–(4.9) are denoted by ${}^{(1)}G_{L,j}^{a,b,\alpha,\mu}(x)$ and the numerical solutions from the Gauss quadrature (4.19) are denoted by ${}^{(2)}G_{L,j}^{a,b,\alpha,\mu}(x)$. Let $e_j^{(m)}(x) = {}^{(m)}G_{L,j}^{a,b,\alpha,\mu}(x) - G_{L,j}^{a,b,\alpha,\mu}(x)$ ($m = 1, 2$), where $G_{L,j}^{a,b,\alpha,\mu}(x)$ is the reference solution from the first equation in (4.17) with $\mu = b$. Then the relative L^∞ error is defined by

$$\|e^{(m)}\|_\infty = \frac{\max_{0 \leq j \leq N} \max_{0 \leq k \leq 256} |e_j^{(m)}(x_k)|}{\max_{0 \leq j \leq N} \max_{0 \leq k \leq 256} |G_{L,j}^{a,b,\alpha,\mu}(x_k)|}, \quad x_k = -1 + \frac{2k}{256}.$$

In Table 1, we observe that the recurrence formula (4.8)–(4.9) shows higher accuracy while the Gauss quadrature (4.19) shows less accurate results, especially when

TABLE 1

Comparison between the error $\|e^{(1)}\|_\infty$ of the recurrence formula (4.8)–(4.9) and the error $\|e^{(2)}\|_\infty$ of the JG quadrature (4.19), $a = 0, b = \mu, \alpha(x) = 2|\sin(10x)|$.

N	μ	$\ e^{(1)}\ _\infty$	$\ e^{(2)}\ _\infty$	μ	$\ e^{(1)}\ _\infty$	$\ e^{(2)}\ _\infty$	μ	$\ e^{(1)}\ _\infty$	$\ e^{(2)}\ _\infty$
64	0.2	1.59e-15	2.46e-14	0.5	1.22e-15	2.76e-14	0.8	3.00e-15	2.68e-14
128		1.59e-15	1.67e-13		1.22e-15	1.47e-13		3.34e-15	1.35e-13
256		2.67e-15	7.62e-13		1.22e-15	7.94e-13		3.53e-15	1.53e-12
512		2.67e-15	6.31e-12		1.22e-15	7.63e-12		8.83e-15	8.45e-12
64	-0.2	1.73e-15	1.41e-14	-0.5	2.40e-15	1.04e-14	-0.8	3.16e-15	6.36e-15
128		2.25e-15	1.09e-13		3.39e-15	5.73e-14		5.50e-15	3.66e-14
256		2.32e-15	6.42e-13		4.79e-15	4.10e-13		9.57e-15	1.79e-13
512		5.56e-15	3.88e-12		6.77e-15	4.65e-12		1.66e-14	1.55e-12

N is large. This is possibly due to the accumulation of the round-off errors in the summation in (4.19). Further, the Gauss quadrature (4.19) takes much more time than the recurrence formula (4.8)–(4.9). For fixed x , we need $O(N)$ operations to obtain ${}^{(1)}G_{L,j}^{a,b,\alpha,\mu}(x)$ ($j = 0, 1, \dots, N$), while we need at least $O(N^2)$ operations to obtain ${}^{(2)}G_{L,j}^{a,b,\alpha,\mu}(x)$ ($j = 0, 1, \dots, N$). Moreover, we also need to recalculate the Gauss quadrature points $\{s_k\}$ and weights $\{\omega_k\}$ in (4.19) when x changes, and thus the computational cost is $O(N^3)$. From Table 1, we observe better accuracy of the recurrence formula, which implies the stability of the recurrence formula (4.8)–(4.9).

4.2. Riemann–Liouville fractional derivatives of the weighted Jacobi polynomials. In this subsection, we compute the Riemann–Liouville fractional derivatives of $P_{+,j}^{a,b,\mu}(x)$ and $P_{-,j}^{a,b,u}(x)$. To this end, we adopt the technique used in [16] to get the fractional derivative of $P_{+,j}^{a,b,\mu}(x)$ (or $P_{-,j}^{a,b,\mu}(x)$) from the corresponding fractional integral of $P_{+,j}^{a,b,\mu}(x)$ (or $P_{-,j}^{a,b,\mu}(x)$). For simplicity, we denote

$$(4.20) \quad {}_{RL}S_{L,j}^{a,b,\alpha,\mu}(x) = {}_{RL}D_{-1,x}^{\alpha(x)}P_{+,j}^{a,b,\mu}(x), \quad {}_{RL}S_{R,j}^{a,b,\alpha,\mu}(x) = {}_{RL}D_{x,1}^{\alpha(x)}P_{-,j}^{a,b,\mu}(x).$$

In the rest of this subsection, we use $S_{L,j}(x) = {}_{RL}S_{L,j}^{a,b,\alpha,\mu}(x)$ and $S_{R,j}(x) = {}_{RL}S_{R,j}^{a,b,\alpha,\mu}(x)$ for simplicity.

When $\alpha(x) = \alpha$ is a constant and $n - 1 < \alpha < n, n \in \mathbb{N}$, we have

$$S_{L,j}(x) = \frac{d^n}{dx^n}G_{L,j}^{a,b,n-\alpha,\mu}(x), \quad S_{R,j}(x) = (-1)^n \frac{d^n}{dx^n}G_{R,j}^{a,b,n-\alpha,\mu}(x).$$

For $0 < \alpha < 1$, letting $\tilde{\alpha} = 1 - \alpha$ and $s = (x + 1)\hat{s} - 1$, we have

$$\begin{aligned} S_{L,j}(x) &= \frac{d}{dx}G_{L,j}^{a,b,\tilde{\alpha},\mu}(x) = \frac{(x + 1)^{\tilde{\alpha}+\mu}}{\Gamma(\tilde{\alpha})} \int_0^1 (1 - \hat{s})^{\tilde{\alpha}-1} \hat{s}^{\mu+1} \frac{\partial P_j^{a,b}(s)}{\partial s} d\hat{s} \\ &\quad + \frac{\tilde{\alpha} + \mu}{x + 1} \frac{(x + 1)^{\tilde{\alpha}+\mu}}{\Gamma(\tilde{\alpha})} \int_0^1 (1 - \hat{s})^{\tilde{\alpha}-1} \hat{s}^\mu P_j^{a,b}(s) d\hat{s}, \end{aligned}$$

which leads to

$$(4.21) \quad S_{L,j}(x) = \frac{1}{x + 1} \left((\tilde{\alpha} + \mu)G_{L,j}^{a,b,\tilde{\alpha},\mu}(x) + d_{j,1}^{a,b}G_{L,j-1}^{a+1,b+1,\tilde{\alpha},\mu+1}(x) \right),$$

where we have used $\frac{dP_j^{a,b}(x)}{dx} = d_{j,1}^{a,b}P_{j-1}^{a,b}(x)$ and $d_{j,1}^{a,b}$ is defined by (A.3).

For $1 < \alpha < 2$, letting $\tilde{\alpha} = 2 - \alpha$ and $s = (x + 1)\hat{s} - 1$, we have

$$\begin{aligned} S_{L,j}(x) &= \frac{d^2}{dx^2} G_{L,j}^{a,b,\tilde{\alpha},\mu}(x) = \frac{(x+1)^{\tilde{\alpha}+\mu}}{\Gamma(\tilde{\alpha})} \int_0^1 (1-\hat{s})^{\tilde{\alpha}-1} \hat{s}^{\mu+2} \frac{\partial^2 P_j^{a,b}(s)}{\partial s^2} d\hat{s} \\ &\quad + \frac{2(\alpha+\mu)}{x+1} \frac{(x+1)^{\tilde{\alpha}+\mu}}{\Gamma(\tilde{\alpha})} \int_0^1 (1-\hat{s})^{\tilde{\alpha}-1} \hat{s}^{\mu+1} \frac{\partial P_j^{a,b}(s)}{\partial s} d\hat{s} \\ &\quad + \frac{(\tilde{\alpha}+\mu)(\tilde{\alpha}+\mu-1)}{(x+1)^2} \frac{(x+1)^{\tilde{\alpha}+\mu}}{\Gamma(\tilde{\alpha})} \int_0^1 (1-\hat{s})^{\tilde{\alpha}-1} \hat{s}^{\mu} P_j^{a,b}(s) d\hat{s}. \end{aligned}$$

Applying (A.2) and (A.3) (see appendix) with $n = 1, 2$, we obtain

$$\begin{aligned} (4.22) \quad S_{L,j}(x) &= \frac{1}{(x+1)^2} \left[(\tilde{\alpha}+\mu)(\tilde{\alpha}+\mu-1) G_{L,j}^{a,b,\tilde{\alpha},\mu}(x) \right. \\ &\quad \left. + 2(\tilde{\alpha}+\mu) d_{j,1}^{a,b} G_{L,j-1}^{a+1,b+1,\tilde{\alpha},\mu+1}(x) + d_{j,2}^{a,b} G_{L,j-2}^{a+2,b+2,\tilde{\alpha},\mu+2}(x) \right]. \end{aligned}$$

When $\alpha(x)$ is a function of $x, x \in (-1, 1]$, we can readily verify that (4.21) and (4.22) hold from the definitions (2.3) and (2.4). Also, when $\alpha(x) > 2$, $S_{L,j}(x)$ can be similarly derived, which is omitted here.

For the right fractional derivative operator, we have similar relations. For a given $x \in [-1, 1]$ and $0 < \alpha(x) < 1$, letting $\tilde{\alpha}(x) = 1 - \alpha(x)$, we have

$$(4.23) \quad S_{R,j}(x) = \frac{1}{1-x} \left((\tilde{\alpha}+\mu) G_{R,j}^{a,b,\tilde{\alpha},\mu}(x) - d_{j,1}^{a,b} G_{R,j-1}^{a+1,b+1,\tilde{\alpha},\mu+1}(x) \right).$$

For a given $x \in [-1, 1]$ and $1 < \alpha(x) < 2$, let $\tilde{\alpha}(x) = 2 - \alpha(x)$ and we have

$$\begin{aligned} (4.24) \quad S_{R,j}(x) &= \frac{1}{(1-x)^2} \left[(\tilde{\alpha}+\mu)(\tilde{\alpha}+\mu-1) G_{R,j}^{a,b,\tilde{\alpha},\mu}(x) \right. \\ &\quad \left. - 2(\tilde{\alpha}+\mu) d_{j,1}^{a,b} G_{R,j-1}^{a+1,b+1,\tilde{\alpha},\mu+1}(x) + d_{j,2}^{a,b} G_{R,j-2}^{a+2,b+2,\tilde{\alpha},\mu+2}(x) \right]. \end{aligned}$$

4.3. Differentiation matrices of the Riemann–Liouville fractional derivatives. Let $u(x) = (1 \pm x)^\mu v(x)$ be a function defined on the interval $[-1, 1]$ and N be a positive integer. Denote $x_j (j = 0, 1, \dots, N)$ as the JGL points defined on the interval $[-1, 1]$. Then $u(x)$ can be approximated by

$$(4.25) \quad I_N^{\mu,a,b,\pm} u(x) = (1 \pm x)^\mu I_N^{a,b} v(x) = (1 \pm x)^\mu \sum_{j=0}^N v(x_j) l_j(x) = \sum_{j=0}^N \hat{v}_j P_{\pm,j}^{a,b,\mu}(x),$$

where $l_j(x)$ is the Lagrange interpolation basis function based on JGL points and $l_j(x)$ can be represented as

$$(4.26) \quad l_j(x) = \sum_{k=0}^N c_{k,j} P_k^{a,b}(x).$$

Then $c_{k,j}$ can be determined by the following relation [28]

$$(4.27) \quad (\mathcal{C})_{k,j} = c_{k,j} = \frac{P_k^{a,b}(x_j) \omega_j}{\delta_k \gamma_k^{a,b}}, \quad k = 0, 1, \dots, N,$$

in which $\gamma_k^{a,b}$ is defined by (4.5), $\delta_k = 1$ ($0 \leq k < N$), and $\delta_N = 2 + \frac{a+b+1}{N}$. If $I_N^{a,b}$ in (4.25) is the JG or Jacobi–Gauss–Radau (JGR) interpolation, then we have $\delta_k = 1$ ($0 \leq k \leq N$) in (4.27). Combining (4.26)–(4.27) yields

$$(4.28) \quad \hat{\mathbf{v}} = \mathcal{C}\mathbf{v}(\mathbf{x}),$$

where $\hat{\mathbf{v}} = (\hat{v}_0, \hat{v}_1, \dots, \hat{v}_N)^T$ and $\mathbf{v}(\mathbf{x}) = (v(x_0), v(x_1), \dots, v(x_N))^T$.

The Riemann–Liouville derivative ${}_{RL}D_{-1,x}^{\alpha(x)} I_N^{\mu,a,b,+} u(x)$ ($\alpha(x) > 0, x \in [-1, 1]$) can be calculated by the following relation

$$(4.29) \quad {}_{RL}D_{-1,x}^{\alpha(x)} I_N^{\mu,a,b,+} u(x) = \sum_{j=0}^N \hat{v}_j {}_{RL}S_{L,j}^{a,b,\alpha,\mu}(x),$$

where ${}_{RL}S_{L,j}^{a,b,\alpha,\mu}(x)$ is defined in (4.20). Combining (4.28) and (4.29) yields

$$(4.30) \quad {}_{RL}D_{-1,x}^{\alpha(x)} I_N^{\mu,a,b,+} u(x) = \left({}_{RL}S_{L,0}^{a,b,\alpha,\mu}(x), {}_{RL}S_{L,1}^{a,b,\alpha,\mu}(x), \dots, {}_{RL}S_{L,N}^{a,b,\alpha,\mu}(x) \right) \mathcal{C}\mathbf{v}(\mathbf{x}).$$

Let ${}_{RL}D_{-1,x_j}^{\alpha(x_j)} I_N^{\mu,a,b,+} u(x_j) = [{}_{RL}D_{-1,x}^{\alpha(x)} I_N^{\mu,a,b,+} u(x)]_{x=x_j}$. Then ${}_{RL}D_{-1,x}^{\alpha(x)} I_N^{\mu,a,b,+} u$ at the collocation points $x = x_j$ ($j = 0, 1, \dots, N$) can be calculated by the following simple formula

$$(4.31) \quad \left({}_{RL}D_{-1,x_0}^{\alpha(x_0)} I_N^{\mu,a,b,+} u(x_0), \dots, {}_{RL}D_{-1,x_N}^{\alpha(x_N)} I_N^{\mu,a,b,+} u(x_N) \right)^T = \mathcal{D}_L \tilde{\mathbf{u}}(\mathbf{x}),$$

where $\tilde{\mathbf{u}}(\mathbf{x}) = (v(x_0), u(x_1), u(x_2), \dots, u(x_N))^T$, $v(x_0) = \lim_{x \rightarrow x_0^+} (x - x_0)^{-\mu} u(x)$, the differential matrix $\mathcal{D}_L = \mathcal{SC} \operatorname{diag}(1, (1+x_1)^{-\mu}, \dots, (1+x_N)^{-\mu})$, the matrix \mathcal{S} satisfies $(\mathcal{S})_{i,j} = {}_{RL}S_{L,j}^{a,b,\alpha,\mu}(x_i)$ ($i, j = 0, 1, \dots, N$), and ${}_{RL}S_{L,j}^{a,b,\alpha,\mu}(x)$ is defined in (4.20).

We can similarly derive the differentiation matrix \mathcal{D}_R such that

$$(4.32) \quad \left({}_{RL}D_{x_0,1}^{\alpha(x_0)} I_N^{\mu,a,b,-} u(x_0), \dots, {}_{RL}D_{x_N,1}^{\alpha(x_N)} I_N^{\mu,a,b,-} u(x_N) \right)^T = \mathcal{D}_R \hat{\mathbf{u}}(\mathbf{x}),$$

where $\hat{\mathbf{u}}(\mathbf{x}) = (u(x_0), u(x_1), \dots, u(x_{N-1}), v(x_N))^T$, $v(x_N) = \lim_{x \rightarrow x_N^-} (x_N - x)^{-\mu} u(x)$, $\mathcal{D}_R = \mathcal{SC} \operatorname{diag}((1-x_0)^{-\mu}, (1-x_1)^{-\mu}, \dots, (1-x_{N-1})^{-\mu}, 1)$, the matrix \mathcal{S} satisfies $(\mathcal{S})_{i,j} = {}_{RL}S_{R,j}^{a,b,\alpha,\mu}(x_i)$ ($i, j = 0, 1, \dots, N$), and ${}_{RL}S_{R,j}^{a,b,\alpha,\mu}(x)$ is defined in (4.20).

We can similarly derive the differentiation matrices based on the JG and JGR points. For example, when the JG points are used, the right-hand side in (4.31) is replaced by $\mathcal{D}_L \mathbf{u}(\mathbf{x})$, where $\mathcal{D}_L = \mathcal{SC} \operatorname{diag}((1+x_0)^{-\mu}, (1+x_1)^{-\mu}, \dots, (1+x_N)^{-\mu})$.

4.4. Differentiation matrices of the Caputo fractional derivatives. In this subsection, we focus on the computation of ${}_C S_{L,j}^{a,b,\alpha,\mu}(x) = {}_C D_{-1,x}^{\alpha(x)} P_{j,+}^{a,b,\mu}(x)$ and ${}_C S_{R,j}^{a,b,\alpha,\mu}(x) = {}_C D_{x,1}^{\alpha(x)} P_{j,-}^{a,b,\mu}(x)$, which leads to the desired differentiation matrices of the Caputo fractional derivatives. In the rest of this subsection, we also use $S_{L,j}(x) = {}_C S_{L,j}^{a,b,\alpha,\mu}(x)$ and $S_{R,j}(x) = {}_C S_{R,j}^{a,b,\alpha,\mu}(x)$ for simplicity.

For $\mu \geq 0$ and $0 < \alpha(x) < 1$ with $\tilde{\alpha} = 1 - \alpha$, we have

$$\begin{aligned} S_{L,j}(x) &= {}_C D_{-1,x}^{\alpha(x)} P_{j,+}^{a,b,\mu}(x) \\ &= \frac{1}{\Gamma(\tilde{\alpha})} \int_{-1}^x (x-s)^{\tilde{\alpha}-1} \left[\mu(1+s)^{\mu-1} P_j^{a,b}(s) + d_{j,1}^{a,b}(1+s)^\mu P_{j-1}^{a+1,b+1}(s) \right] ds, \end{aligned}$$

which leads to

$$(4.33) \quad S_{L,j}(x) = \mu G_{L,j}^{a,b,1-\alpha,\mu-1}(x) + d_{j,1}^{a,b} G_{L,j-1}^{a+1,b+1,1-\alpha,\mu}(x).$$

Similarly, we have

$$(4.34) \quad S_{R,j}(x) = \mu G_{R,j}^{a,b,1-\alpha,\mu-1}(x) - d_{j,1}^{a,b} G_{R,j-1}^{a+1,b+1,1-\alpha,\mu}(x), \quad 0 < \alpha(x) < 1.$$

For $\mu \geq 1$ and $1 < \alpha < 2$, we obtain

$$\begin{aligned} (4.35) \quad S_{L,j}(x) &= \mu(\mu-1)G_{L,j}^{a,b,2-\alpha,\mu-2}(x) + 2\mu d_{j,1}^{a,b} G_{L,j-1}^{a+1,b+1,2-\alpha,\mu-1}(x) \\ &\quad + d_{j,2}^{a,b} G_{L,j-2}^{a+2,b+2,2-\alpha,\mu}(x), \\ (4.36) \quad S_{R,j}(x) &= \mu(\mu-1)G_{R,j}^{a,b,2-\alpha,\mu-2}(x) - 2\mu d_{j,1}^{a,b} G_{R,j-1}^{a+1,b+1,2-\alpha,\mu-1}(x) \\ &\quad + d_{j,2}^{a,b} G_{R,j-2}^{a+2,b+2,2-\alpha,\mu}(x). \end{aligned}$$

Remark 4.2. According to (2.7), we can also calculate the Caputo derivative ${}_C D_{-1,x}^{\alpha(x)} P_{+,j}^{a,b,\mu}(x)$ (or ${}_C D_{x,1}^{\alpha(x)} P_{-,j}^{a,b,\mu}(x)$) from ${}_R L D_{-1,x}^{\alpha(x)} P_{+,j}^{a,b,\mu}(x)$ (or ${}_R L D_{x,1}^{\alpha(x)} P_{-,j}^{a,b,\mu}(x)$).

Remark 4.3. When $\mu = 0$, we have (cf. [16, 40] where $\alpha(x)$ is a constant)

$$(4.37) \quad {}_C S_{L,j}^{a,b,\alpha,0}(x) = {}_C D_{-1,x}^{\alpha(x)} P_{j,+}^{a,b,0}(x) = d_{j,n}^{a,b} G_{L,j-n}^{a+n,b+n,n-\alpha,0}(x),$$

$$(4.38) \quad {}_C S_{R,j}^{a,b,\alpha,0}(x) = {}_C D_{x,1}^{\alpha(x)} P_{j,-}^{a,b,0}(x) = (-1)^n d_{j,n}^{a,b} G_{R,j-n}^{a+n,b+n,n-\alpha,0}(x),$$

where $n-1 < \alpha(x) < n$, $n \in \mathbb{N}$, $d_{j,n}^{a,b}$ is defined by (A.3), and $G_{L,j}^{a,b,\alpha,\mu}(x)$ and $G_{R,j}^{a,b,\alpha,\mu}(x)$ are defined by (4.6) and (4.7), respectively.

For the Caputo derivatives, we can similarly derive the following differentiation matrices $\mathcal{D}_L, \mathcal{D}_R \in \mathbb{R}^{(N+1) \times (N+1)}$ such that

$$(4.39) \quad \left({}_C D_{-1,x_0}^{\alpha(x_0)} I_N^{\mu,a,b,+} u(x_0), \dots, {}_C D_{-1,x_N}^{\alpha(x_N)} I_N^{\mu,a,b,+} u(x_N) \right)^T = \mathcal{D}_L \mathbf{u}(\mathbf{x}),$$

$$(4.40) \quad \left({}_C D_{x_0,1}^{\alpha(x_0)} I_N^{\mu,a,b,-} u(x_0), \dots, {}_C D_{x_N,1}^{\alpha(x_N)} I_N^{\mu,a,b,-} u(x_N) \right)^T = \mathcal{D}_R \mathbf{u}(\mathbf{x}).$$

Remark 4.4. The total computational cost of the present algorithm is $O(N^3)$, where $N \times N$ is the size of the fractional differentiation matrices. For the differentiation matrices based on the Chebyshev–Gauss–Lobatto points, the computational cost can be reduced to $O(N^2 \log N)$ due to the fast Fourier transform. In the standard spectral collocation method, i.e., $\alpha = 1, 2$, we have the exact formula to calculate the differentiation matrices with $O(N^2)$ operations; see [28].

5. Applications and numerical examples. In this section, we first illustrate the spectral collocation method proposed in section 2 to solve FODEs and compare the numerical results with existing spectral collocation methods. Then we illustrate the spectral collocation methods to solve FPDEs.

We will present three examples. In the first two examples, the endpoint singularity index of solution is known, and we mainly focus on the convergence order of our methods and test the methods for different situations. In the third example, we consider a fractional Burgers equations where the endpoint singularity index of the solution is not explicitly known.

TABLE 2
Maximum errors for Example 5.1 for Case I, $\mu = 0$.

	N	(a, b)	Error	(a, b)	Error	(a, b)	Error
Case I	4	(0,0)	2.3866e-01	$(-\frac{1}{2}, -\frac{1}{2})$	2.9661e-01	$(-\frac{1}{2}, \frac{1}{2})$	6.9196e-01
	8		1.3750e-03		1.5597e-03		2.8386e-03
	16		7.9171e-11		4.8886e-11		3.2089e-10
	32		3.4348e-15		5.1070e-15		6.7724e-15
	64		3.7541e-15		3.8858e-15		7.7091e-15

Example 5.1. Solve FODE (3.1) with $x \in (0, 1]$ and the following conditions:

- Case I (smooth solution): Choose the suitable initial condition and the right-hand side function $f(x)$, such that the analytical solution to (3.1) is $u(x) = \sin(2\pi x)$, where $C(x) = \frac{1}{1+x^2}$ and $\alpha(x) = \frac{1}{\sin^2(10x)+1.1}$.
- Case II (solution with endpoint singularity): We choose $C(x) = 0$, $\alpha = \alpha(x)$ is a constant, and $f(x)$ is chosen as $f(x) = x^\sigma \sin(x+1)$, $\sigma \geq 0$.
- Case III (solution with endpoint singularity): Choose the suitable initial condition and the right-hand side function $f(x)$, such that the analytical solution to (3.1) is¹ $u(x) = x^\sigma + x^{2\sigma}$, $\sigma > 0$, where $C(x) = \frac{1}{1+x^2}$ and $\alpha(x) = |x - \frac{1}{2}| + \frac{1}{3}$.

In this example, the errors are measured in the following sense:

$$\|e\|_\infty = \max_{1 \leq j \leq K} |u_{\text{ref}}(z_j) - \tilde{u}(z_j)|, \quad z_j = j/K, \quad j = 0, 1, \dots, K, \quad K = 128,$$

where $\tilde{u}(x) = x^\mu \sum_{j=0}^N v_j l_j(x)$, $l_j(x)$ is the Lagrange basis function based on JGL points on the interval $[0, 1]$, and u_{ref} is either the exact solution or a numerical solution obtained from JGL collocation method (3.2) with $N = 128$.

In Case I, the solution is smooth and then we use (3.3) with $\mu = 0$ (standard spectral collocation method; see, e.g., [31]) to solve it. In Table 2, we observe spectral accuracy for the smooth solutions when three types of collocation points are used. For the same N , the three sets of collocation points give the same level of accuracy, which is expected from standard spectral theory; see, e.g., [14].

For Case II, we know from [44] that the analytical solution $u(x)$ to (3.1) satisfies $u(x) = x^{\sigma+\alpha-\lfloor\sigma+\alpha\rfloor} v(x)$ or $u(x) = x^{\sigma+\alpha-\lceil\sigma+\alpha\rceil} v(x)$ when $f(x) = x^\sigma \sin(x+1)$, where $v(x) \in H^\infty([0, 1])$. Here, we apply the JGL collocation method (3.3) with three choices of μ : $\mu = \sigma + \alpha - \lfloor\sigma + \alpha\rfloor$ ($-1 < \mu \leq 0$), $\mu = \sigma + \alpha - \lceil\sigma + \alpha\rceil$ ($0 \leq \mu < 1$), and $\mu = 0$. As we do not have the exact solution, we use the reference solution u_{ref} obtained by (3.3) with $N = 128$ JGL collocation points for each group of parameters $\sigma, \alpha, \mu, a, b$ (see also the values of these parameters in Tables 3–4). In Table 3,² we show the errors $\|e\|_\infty$ by using the Legendre–Gauss–Lobatto (LGL) spectral collocation method ($a = b = 0$), and the errors $\|e\|_\infty$ of the Chebyshev–Gauss–Lobatto collocation method ($a = b = -1/2$) are shown in Table 4.

In both tables, we observe spectral accuracy when we choose $\mu = \sigma + \alpha - \lfloor\sigma + \alpha\rfloor$ or $\mu = \sigma + \alpha - \lceil\sigma + \alpha\rceil$ for $\sigma + \alpha \geq 1$. Note that we are actually approximating v instead of u . While we have a smooth v with the chosen parameter μ , it is natural to expect spectral accuracy. However, it is still important to choose $\mu < 0$ if JGL collocation methods are used. When $0 < \sigma + \alpha < 1$, we choose $\mu = \sigma + \alpha - \lceil\sigma + \alpha\rceil$ ($-1 < \mu < 0$),

¹Here we choose such a solution to somewhat mimic the singularity structure of the solution of ${}_CD_{0,x}^\alpha u + u = 1$, $u(0) = u_0$, $0 < \alpha < 1$, which is of the form $\sum_{i,j=0}^n c_{i,j} x^{i\alpha+j}$.

²In this table and in Tables 4 and 5, we marked the optimal μ with μ^* for Cases II and III.

TABLE 3
Maximum errors for Example 5.1, Case II, $a = b = 0$.

σ	α	μ	$N = 4$	$N = 8$	$N = 16$	$N = 32$	$N = 64$
0.2	0.2	-0.6*	5.8111e-04	1.9957e-09	5.8564e-15	1.0464e-14	4.8850e-15
		0.4	1.6663e-01	9.7900e-02	4.2005e-02	1.0171e-02	2.9030e-03
		0	1.1811e-01	7.1457e-02	2.5294e-02	3.0128e-03	4.8583e-04
0.8	0.5	-0.7*	2.7865e-04	2.6968e-10	8.2522e-14	6.2637e-14	8.7576e-14
		0.3*	4.8338e-05	8.0547e-11	1.4433e-15	1.7764e-15	1.5543e-15
		0	3.0484e-03	6.3265e-04	1.0778e-04	4.0644e-06	3.6246e-07
1.7	0.8	-0.5*	9.9532e-03	1.4705e-07	1.7592e-14	1.4373e-14	2.0317e-14
		0.5*	2.0276e-05	1.8398e-11	7.7716e-16	1.9429e-15	1.1102e-15
		0	2.8684e-04	1.9274e-05	6.9531e-07	1.2071e-08	3.1498e-10

TABLE 4
Maximum errors for Example 5.1, Case II, $a = b = -1/2$.

σ	α	μ	$N = 4$	$N = 8$	$N = 16$	$N = 32$	$N = 64$
0.2	0.2	-0.6*	4.8717e-04	1.3141e-09	1.8874e-15	3.3029e-15	2.4425e-15
		0.4	1.5900e-01	9.3274e-02	3.2727e-02	1.4969e-02	6.3009e-03
		0	1.1388e-01	6.6410e-02	1.5528e-02	4.2654e-03	1.3560e-03
0.8	0.5	-0.7*	2.3305e-04	1.8148e-10	1.2456e-14	1.9332e-14	2.8945e-14
		0.3*	7.2505e-05	1.1160e-10	9.9920e-16	7.7716e-16	1.4433e-15
		0	2.7518e-03	5.1459e-04	7.0073e-05	3.9047e-06	2.0670e-07
1.7	0.8	-0.5*	8.2223e-03	9.2855e-08	1.1102e-15	1.6567e-15	7.0679e-15
		0.5*	2.8742e-05	2.5962e-11	7.7716e-16	1.1657e-15	1.9429e-15
		0	1.9856e-04	1.3396e-05	4.3241e-07	5.7959e-09	1.2829e-10

TABLE 5
Maximum errors for Example 5.1, Case III, $a = -\mu, b = \mu$.

σ	μ	$N = 4$	$N = 8$	$N = 16$	$N = 32$	$N = 64$
1.3	-0.7*	5.4992e-04	1.0523e-05	2.5302e-07	5.9610e-09	1.3223e-10
	-0.4	2.5433e-03	3.9183e-04	5.2868e-05	7.0554e-06	8.3719e-07
	0	4.7920e-03	1.2883e-03	2.5965e-04	2.8371e-05	3.5713e-06
1.5	-0.5*	6.2021e-04	5.6469e-06	7.6852e-08	1.0087e-09	1.2946e-11
	-0.55	3.9389e-04	2.4162e-05	3.3420e-06	3.5877e-07	3.3376e-08
	0	4.4015e-03	8.0197e-04	1.2153e-04	9.8811e-06	9.8474e-07
1.8	-0.2*	4.4378e-04	2.0038e-06	1.2603e-08	6.1470e-11	3.2969e-13
	-0.3	2.3472e-04	3.9786e-05	2.7610e-06	1.7865e-07	1.1111e-08
	0	2.1472e-03	1.8291e-04	1.8154e-05	9.4600e-07	6.5811e-08

where we still observe spectral accuracy; see the text before Remark 3.1 for choosing μ . However, if $0 < \sigma + \alpha < 1$ and we choose $\mu = \sigma + \alpha > 0$, then we need to know $v(0)$ to recover spectral accuracy and observe otherwise only slow convergence. When we simply take $v(0)$ any value other than the exact value (here the exact value of $v(0)$ is $\frac{\Gamma(\sigma+1)}{\Gamma(\sigma+1+\alpha)} \sin(1)$), we cannot observe spectral accuracy; see (3.3), and Tables 3–4 where $v(0) = 0$ is used whenever $0 < \mu = \sigma + \alpha < 1$. If $0 < \mu = \sigma + \alpha < 1$ is chosen, then one can use JG points to avoid the dilemma instead of JGL points (see [44]), where the solutions are evaluated only at interior points.

For Case III, we observe in Table 5 that higher accuracy is obtained when $\mu < 0$ as we can expect from the fact $v(x) = x^{-\mu} u(x)$ has better regularity than $u(x)$ ($\mu = 0$). We observe that the best choice of μ is $\mu = \sigma - \lceil \sigma \rceil < 0$.

Next, we apply the spectral collocation methods to solve space-time FPDEs and test these methods when solutions are known and smooth.

Example 5.2. Consider the following space-time-fractional advection-diffusion equation over $(-1, 1) \times (0, 1]$ (see, e.g., [38]):

$$(5.1) \quad \begin{cases} {}_C D_{0,t}^{\gamma(x,t)} u(x,t) + {}_{RL} D_{-1,x}^{\beta(x,t)} u(x,t) = {}_{RL} D_{-1,x}^{\alpha(x,t)} u(x,t) + f(x,t), \\ u(x,0) = 0, \quad x \in [-1, 1], \\ u(-1,t) = u(1,t) = 0, \quad t \in (0, 1], \end{cases}$$

where $0 < \gamma(x,t), \beta(x,t) < 1$ and $1 < \alpha(x,t) < 2$.

We represent the solution $u(x,t)$ to (5.1) as $u(x,t) = t^\mu (x - x_L)^\sigma v(x,t)$. We interpolate $v(x,t)$ on the JGL points (x_j, t_k) , where

$$(5.2) \quad x_j = \frac{x_R - x_L}{2} \hat{x}_j + \frac{x_L + x_R}{2}, \quad t_k = \frac{T(\hat{t}_k + 1)}{2}.$$

Here $\{\hat{x}_j\}$ and $\{\hat{t}_k\}$ are the roots of $(1 - x^2)(P_N^{a_1, b_1}(x))'$ and $(1 - t^2)(P_M^{a_2, b_2}(t))'$, respectively. Hence $u(x,t)$ can be approximated by $I_{M,N}^{\mu, \sigma, a_1, b_1, a_2, b_2, +} u(x,t) = t^\mu (x - x_L)^\sigma I_{M,N}^{a_1, b_1, a_2, b_2} v(x,t) = t^\mu (x - x_L)^\sigma \sum_{j=0}^N \sum_{k=0}^M v_{j,k} l_j(x) h_k(t)$, $l_j(x)$ and $h_k(t)$ are Lagrange interpolation polynomials. Replacing $u(x,t)$ in (5.1) with $I_{M,N}^{\mu, \sigma, a_1, b_1, a_2, b_2, +} u$ and letting $(x,t) = (x_j, t_k)$ yields

$$(5.3) \quad \begin{cases} \left[{}_C D_{0,t}^{\gamma(x_j,t)} I_{M,N}^{\mu, \sigma, a_1, b_1, a_2, b_2, +} u(x_j, t) \right]_{t=t_k} = \left[{}_{RL} D_{x_L, x}^{\alpha(x,t_k)} I_{M,N}^{\mu, \sigma, a_1, b_1, a_2, b_2, +} u(x, t_k) \right]_{x=x_j} \\ \quad + \left[{}_{RL} D_{x_L, x}^{\beta(x,t_k)} I_{M,N}^{\mu, \sigma, a_1, b_1, a_2, b_2, +} u(x, t_k) \right]_{x=x_j} + f(x_j, t_k), \\ \quad j = 1, 2, \dots, N-1, k = 1, 2, \dots, M, \\ u_{j,0} = 0, \quad j = 0, 1, \dots, N, \\ u_{0,k} = 0, \quad u_{N,k} = \psi(t_k), \quad k = 0, 1, \dots, M. \end{cases}$$

In our computation, we take $x_L = -1, x_R = 1, T = 1$, and choose proper $f(x,t)$ such that (5.1) has the exact solution $u(x,t) = t^{6+2/3} \sin(\pi x)$ with different variable-orders given by

- Case I: $\gamma = \beta = \frac{5+4x}{10} \frac{1+4t}{10}$, $\alpha = 1 + \frac{1+4t}{10}$;
- Case II: $\gamma = \frac{1}{|\sin(\pi(x-t))|+1.2}$, $\beta = \frac{|xt|+1}{4}$, $\alpha = \exp(-|xt| - 0.1) + 1$.

The relative L^∞ error is defined by

$$\|e\|_\infty = \frac{\max_{0 \leq j \leq N} \max_{0 \leq k \leq M} |u(x_j, t_k) - u_{i,k}|}{\max_{0 \leq j \leq N} \max_{0 \leq k \leq M} |u_{i,k}|},$$

where (x_j, t_k) are the LGL points from (5.2), i.e., the LGL spectral collocation method is applied in the computation ($a_1 = b_1 = a_2 = b_2 = 0$ in (5.3)). Since the analytical solution is smooth in space, we choose $\sigma = 0$ in (5.3). In Figures 1(a)–(b), we observe machine accuracy when $M \geq 6, \mu = 2/3$ or $M > 6, \mu = -1/3$. This is because the analytical solution $u(x,t)$ to (5.1) satisfies $u(x,t) = t^{2/3} v(x,t)$ or $u(x,t) = t^{-1/3} v(x,t)$, where $v(x,t) = t^6 \sin(\pi x)$ or $t^7 \sin(\pi x)$. When we choose $\mu = 2/3$ or $\mu = -1/3$, we interpolate $v(x,t)$ instead of $u(x,t)$, which yields much higher accuracy due to the smoothness of $v(x,t)$, thus higher accurate numerical solutions of $u(x,t)$.

Conservation laws that involve fractional Laplacians have been widely applied in several fields; see, e.g., [7, 8, 9]. Here, we apply our collocation method to solve a suitable benchmark problem, namely, the space-fractional Burgers equation where the solution is not known explicitly. Numerical results show the superiority of choosing μ close to -1 .

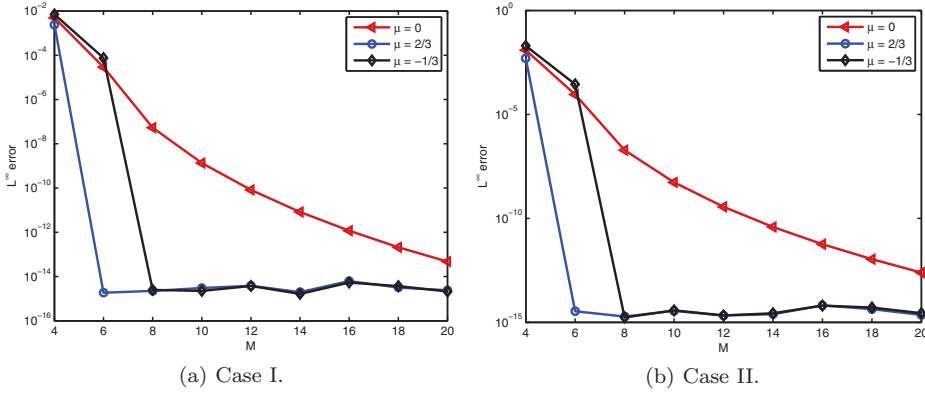


FIG. 1. The relative L^∞ errors for Example 5.2, $N = 24$, $a_1 = b_1 = a_2 = b_2 = 0$.

Example 5.3. Consider the following space-fractional Burgers equation

$$(5.4) \quad \partial_t u(x, t) + u(x, t) \partial_x u(x, t) = \epsilon_{RL} D_{-1,x}^{\alpha(x,t)} u(x, t),$$

subject to the homogeneous boundary conditions and initial condition $u(x, 0) = \varphi(x)$, where $\epsilon > 0$, $1 < \alpha(x, t) < 2$, $(x, t) \in (-1, 1) \times (0, 1]$.

We use the present JGL spectral collocation method in space and the first-order backward difference (backward Euler) method in time to solve (5.4). The method is given by the following: Find $I_N^{\mu,a,b,+} u^n(x) = (x - x_L)^\mu \sum_{j=0}^N v_j^n l_j(x)$ ($n \geq 1$) such that

$$(5.5) \quad \begin{cases} \frac{1}{\tau} (u_j^n - u_j^{n-1}) + u_j^n \left[\partial_x I_N^{\mu,a,b,+} u^n(x) \right]_{x=x_j} = \epsilon \left[{}_{RL} D_{x_L,x}^{\alpha(x,t_n)} I_N^{\mu,a,b,+} u^n(x) \right]_{x=x_j} \\ \quad j = 1, 2, \dots, N-1, \\ u_j^0 = \varphi(x_j), \quad j = 0, 1, \dots, N, \\ u_0^n = u_N^n = 0, \quad n = 0, 1, \dots, n_T, \end{cases}$$

where τ is the time step size with $\tau = T/n_T$, $n_T \in \mathbb{N}$, $t_n = n\tau$, $\{x_j\}$ are the roots of $(1 - x^2)(P_N^{a,b}(x))'$. As (5.5) is implicit, we employ the fixed-point iterations to solve the resulting nonlinear system. As in the previous two examples, we observe better accuracy if $-1 < \mu < 0$ rather than $\mu \geq 0$.

In our computation, we take the initial and boundary conditions as $u(x, 0) = \sin(\pi x)$ and $u(-1, t) = u(1, t) = 0$. We also choose different fractional orders $\alpha(x, t)$ in the numerical tests:

- Case 1: (constant fractional orders) $\alpha(x, t) = 1.1, 1.2, 1.3, 1.5, 1.8$;
- Case 2: (monotonic fractional order) $\alpha(x, t) = \frac{5+4x}{10} + 1$;
- Case 3: (monotonic fractional order) $\alpha(x, t) = \frac{5-4x}{10} + 1$;
- Case 4: (nonsmooth fractional order) $\alpha(x, t) = \frac{4}{5} |\sin(10\pi(x-t))| + 1.1$.
- Case 5: (nonsmooth fractional order) $\alpha(x, t) = \frac{8|x_t|+1}{10} + 1$.

In this example, we apply the LGL spectral collocation method, i.e., $a = b = 0$ in (5.5), to solve (5.4), and the time step size $\tau = 10^{-3}$ and $N = 128$.

We first consider Case 1 with constant fractional orders. For each μ , we choose $\alpha = 1.1, 1.2, 1.3, 1.5$, and 1.8 in the computation; the numerical solutions are shown in Figures 2–5. We observe that the numerical solutions near the origin ($x = -1$) have

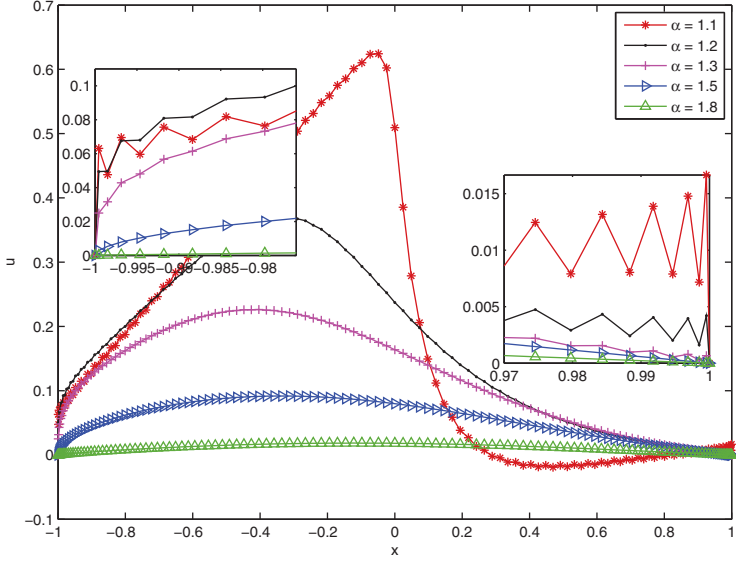


FIG. 2. Numerical solutions of Example 5.3 (Case 1) at $t = 1$ by the method (5.5), $\epsilon = 1$, $a = b = 0$, $N = 128$, $\tau = 10^{-3}$, and $\mu = 0$. The two inset plots show the behavior of the numerical solution near the boundaries.

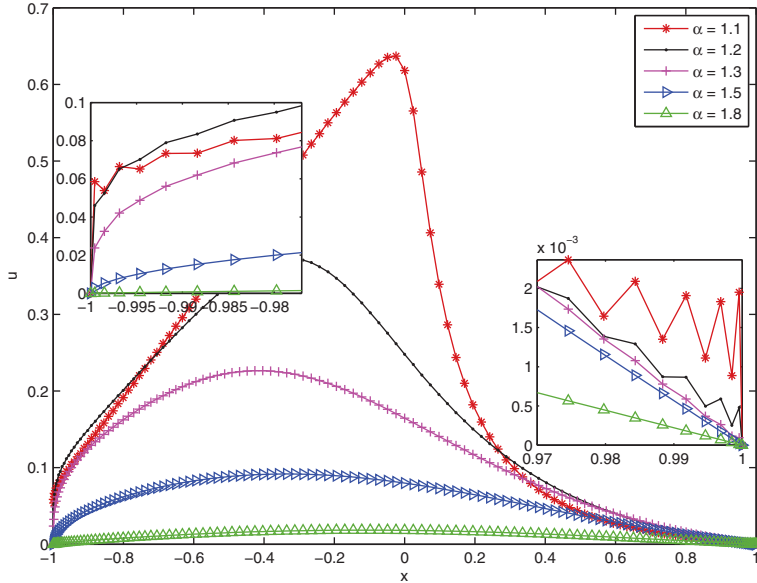


FIG. 3. Numerical solutions of Example 5.3 (Case 1) at $t = 1$ by the method (5.5), $\epsilon = 1$, $a = b = 0$, $N = 128$, $\tau = 10^{-3}$, and $\mu = -0.2$.

a sharp transition, with smaller α leading to sharper transitions; see the magnified subfigures in Figures 2–5. We also observe that smaller μ (see $\mu = -0.45$ in Figure 4 and $\mu = -0.7$ in Figure 5) can capture sharper transitions better than larger μ (see $\mu = 0$ in Figure 2 and $\mu = -0.2$ in Figure 3).

Next, we show numerical solutions for different μ ($\mu = 0, -0.2, -0.45, -0.7, -0.9$) in Figure 6, where we fix $\alpha = 1.1$. We observe that the wiggles are smeared when we

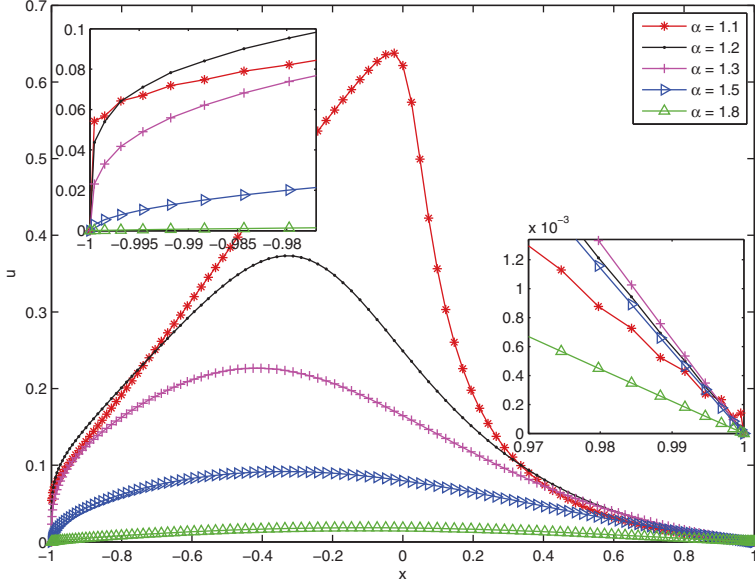


FIG. 4. Numerical solutions of Example 5.3 (Case 1) at $t = 1$ by the method (5.5), $\epsilon = 1$, $a = b = 0$, $N = 128$, $\tau = 10^{-3}$, and $\mu = -0.45$.

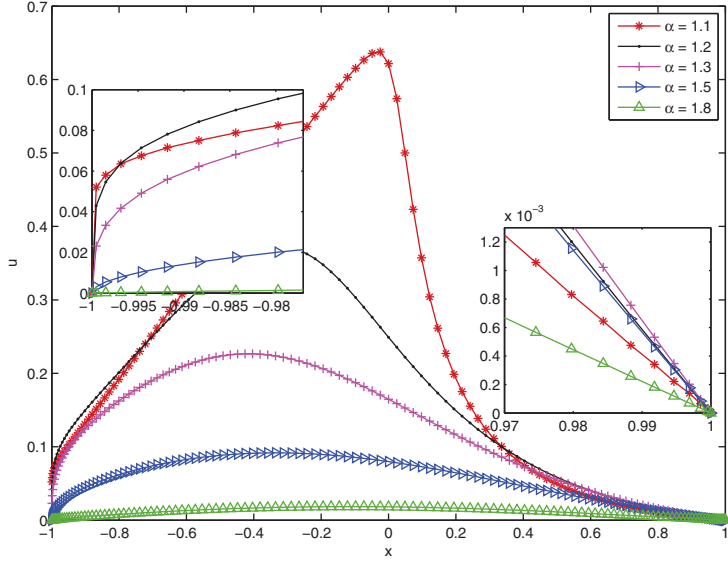


FIG. 5. Numerical solutions of Example 5.3 (Case 1) at $t = 1$ by the method (5.5), $\epsilon = 1$, $a = b = 0$, $N = 128$, $\tau = 10^{-3}$, and $\mu = -0.7$.

have smaller μ ($\mu = 0, -0.2$ versus $\mu = -0.45, -0.7, -0.9$). For $\mu = 0$ and $\mu = -0.2$, numerical solutions are not accurate at endpoints, and this inaccuracy leads to a propagation of errors in the rest of the interval, which is due to the global nature of the fractional differential equations and spectral collocation methods. This suggests that we would have higher accuracy with the proper choices of μ , especially when the solution has an endpoint singularity as in this example.

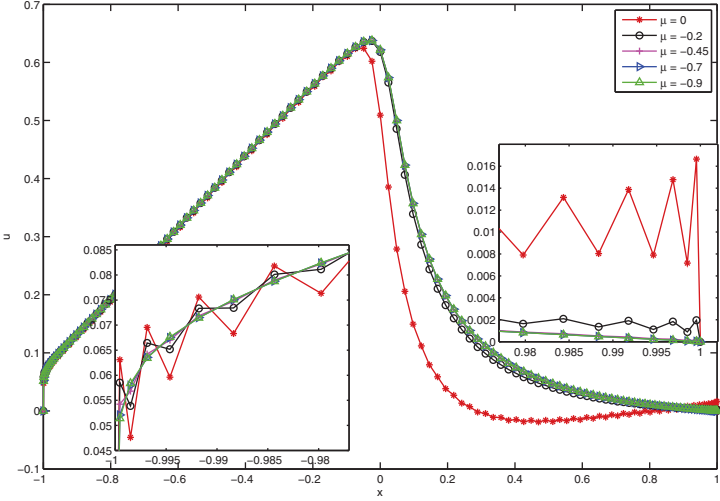


FIG. 6. Numerical solutions of Example 5.3 (Case 1) at $t = 1$, $\alpha = 1.1$, $\epsilon = 1$, $a = b = 0$, $N = 128$, and $\tau = 10^{-3}$.

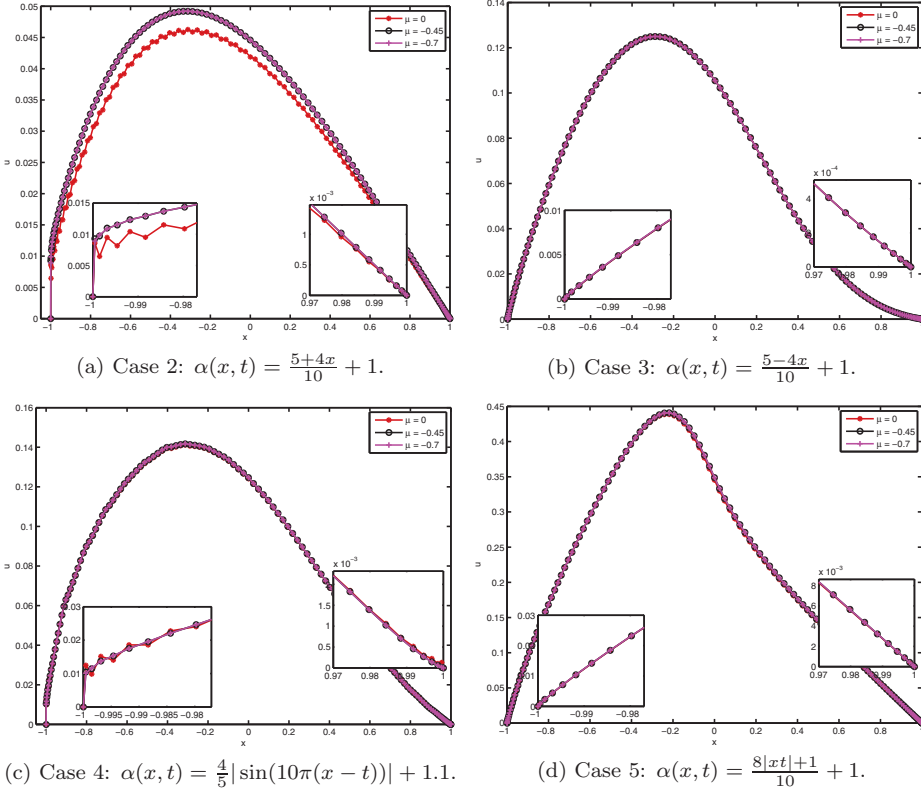


FIG. 7. Numerical solutions of Example 5.3 at $t = 1$, $\epsilon = 1$, $a = b = 0$, $N = 128$, and $\tau = 10^{-3}$.

In Figures 7(a)–(d), we consider Cases 2–5 and we have similar observations: smaller μ leads to better resolution. Also, we observe that when $\alpha(x,t)$ is small at $x = -1$ we need small $\mu < 0$ to get better numerical solutions. For example, in

Figure 7(b) where $\alpha(-1, t) = 1.9$, $\mu = 0$ can lead to a similar resolution as $\mu = -0.45, -0.7$ do while in Figure 7(a), where $\alpha(-1, t) = 1.1$, $\mu = 0$ cannot compete with $\mu = -0.45, -0.7$. We also observe similar effects in Figures 7(c) and 7(d).

6. Conclusion and discussion. In this paper, we proposed the use of the spectral collocation methods using the singular approximation basis functions of the weighted Jacobi polynomials, i.e., $(1 \pm x)^\mu P_j^{a,b}(x)$, $P_j^{a,b}(x)$ is the Jacobi polynomial and $a, b, \mu > -1$, to solve FDEs. We observed that with proper choices of $\mu > -1$, we have better resolution of solutions to constant-order and variable-order FDEs.

When we know exactly the regularity of the exact solutions, we can choose optimal $\mu > -1$ such that higher accuracy can be obtained; see Examples 5.1 and 5.2. When we do not know the regularity of the analytical solutions but still know that the solution has endpoint singularity while the solution is relatively smooth in the interior domain, we always choose suitable $-1 < \mu < 0$ so that higher accuracy can be obtained; see numerical results in section 5.

Compared with the existing works, e.g., [31, 34, 38, 40], we take the weak regularity at the boundary into account in our spectral collocation method to get better resolution at the boundary and thus the whole domain; see Examples 5.1–5.3.

To efficiently evaluate variable-order fractional integrals and derivatives of $(1 \pm x)^\mu P_j^{a,b}(x)$, we developed the recurrence formulas for these integrals and derivatives, which are shown to be numerically stable. In some special cases, the derived recurrence formulas are reduced to the weighted Jacobi polynomials. Comparison with brute force computation of these integrals shows comparable or better accuracy with much improved efficiency.

We will investigate the error estimate of the present spectral collocation methods when regularity of solutions is known and extend the present methods to solve a wider class of FDEs in our future work.

Appendix A. Proofs. Some other properties of the Jacobi polynomials that have been used in the present paper are presented below:

$$(A.1) \quad P_j^{a,b}(1) = \frac{\Gamma(j+a+1)}{j!\Gamma(a+1)}, \quad P_j^{a,b}(-1) = (-1)^j \frac{\Gamma(j+b+1)}{j!\Gamma(b+1)},$$

$$(A.2) \quad \frac{d^n}{dx^n} P_j^{a,b}(x) = d_{j,n}^{a,b} P_{j-n}^{a+n,b+n}(x), \quad j \geq n, n \in \mathbb{N},$$

$$(A.3) \quad d_{j,n}^{a,b} = \frac{\Gamma(j+n+a+b+1)}{2^n \Gamma(j+a+b+1)},$$

$$(A.4) \quad P_j^{a,b}(x) = \frac{d}{dx} \left(\hat{A}_j P_{j-1}^{a,b}(x) + \hat{B}_j P_j^{a,b}(x) + \hat{C}_j P_{j+1}^{a,b}(x) \right), \quad j \geq 1,$$

where \hat{A}_j , \hat{B}_j , \hat{C}_j are from (4.10)–(4.12), respectively.

A.1. Proof of Theorem 4.1.

Proof. For simplicity, we introduce the notation $K_0(x, s) = \frac{1}{\Gamma(\alpha(x))} (x-s)^{\alpha(x)-1} \times (1+s)^\mu$, $K_1(x, s) = (x-s)K_0(x, s)$, and $K_2(x, s) = (1+s)K_1(x, s)$. For $j \geq 1$, we can obtain from the three-term recurrence relation (4.2) that

$$(A.5) \quad \begin{aligned} G_{j+1} &= \int_{-1}^x K_0(x, s) P_{j+1}^{a,b}(s) ds \\ &= \int_{-1}^x K_0(x, s) \left[(A_j s - B_j) P_j^{a,b}(s) - C_j P_{j-1}^{a,b}(s) \right] ds \\ &= (A_j x - B_j) G_j - C_j G_{j-1} - A_j \int_{-1}^x K_1(x, s) P_j^{a,b}(s) ds. \end{aligned}$$

Using $\int_{-1}^x K_1(x, s) P_j^{a,b}(s) ds = H_j$ leads to (4.8). Using the three-term recurrence relation (4.2) again, we have

$$(A.6) \quad \begin{aligned} H_{j+1} &= \int_{-1}^x K_1(x, s) \left[(A_j(s+1) - (A_j + B_j)) P_j^{a,b}(s) - C_j P_{j-1}^{a,b}(s) \right] ds \\ &= A_j \int_{-1}^x K_2(x, s) P_j^{a,b}(s) ds - [(A_j + B_j) H_j + C_j H_{j-1}]. \end{aligned}$$

Let $J(x) = \widehat{A}_j P_{j-1}^{a,b}(x) + \widehat{B}_j P_j^{a,b}(x) + \widehat{C}_j P_{j+1}^{a,b}(x)$. Applying $P_j^{a,b}(x) = \frac{d}{dx} J(x)$ (see (A.4)) yields

$$(A.7) \quad \int_{-1}^x K_2(x, s) P_j^{a,b}(s) ds = - \int_{-1}^x J(s) \frac{\partial}{\partial s} K_2(x, s) ds.$$

Note that $\frac{\partial}{\partial s} K_2(x, s) = (\mu + 1 + \alpha) K_1(x, s) - (1+x)\alpha(x) K_0(x, s)$. So we have

$$(A.8) \quad \begin{aligned} \int_{-1}^x K_2(x, s) P_j^{a,b}(s) ds &= -(\mu + 1 + \alpha(x)) \left(\widehat{A}_j H_{j-1} + \widehat{B}_j H_j + \widehat{C}_j H_{j+1} \right) \\ &\quad + \alpha(x)(1+x) \left(\widehat{A}_j G_{j-1} + \widehat{B}_j G_j + \widehat{C}_j G_{j+1} \right). \end{aligned}$$

Combining (A.6)–(A.8) yields

$$(A.9) \quad \begin{aligned} H_{j+1} &= A_j \left[-(\mu + 1 + \alpha(x)) \left(\widehat{A}_j H_{j-1} + \widehat{B}_j H_j + \widehat{C}_j H_{j+1} \right) \right. \\ &\quad \left. + \alpha(x)(1+x) \left(\widehat{A}_j G_{j-1} + \widehat{B}_j G_j + \widehat{C}_j G_{j+1} \right) \right] \\ &\quad - (A_j + B_j) H_j - C_j H_{j-1}, \end{aligned}$$

which leads to (4.9).

If $\mu = 0$, then we can use (A.4) to obtain

$$(A.10) \quad \begin{aligned} H_j &= \frac{1}{\Gamma(\alpha(x))} \int_{-1}^x (x-s)^{\alpha(x)} P_j^{a,b}(s) ds \\ &= -(x+1)^{\alpha(x)} \frac{J(-1)}{\Gamma(\alpha(x))} + \alpha(x) \frac{1}{\Gamma(\alpha(x))} \int_{-1}^x J(s) (x-s)^{\alpha(x)-1} ds. \end{aligned}$$

Equation (4.15) can be derived directly from (4.8) and (A.10). \square

Theorem 4.2 can be proved similarly and we omit the proof here.

REFERENCES

- [1] A. ATANGANA AND A. H. CLOOT, *Stability and convergence of the space fractional variable-order Schrödinger equation*, Adv. Difference Equ., (2013), 2013:80.
- [2] D. A. BENSON, S. W. WHEATCRAFT, AND M. M. MEERSCHAERT, *Application of a fractional advection-dispersion equation*, Water Resour. Res., 36 (2000), pp. 1403–1412.
- [3] J. CAO AND C. XU, *A high order schema for the numerical solution of the fractional ordinary differential equations*, J. Comput. Phys., 238 (2013), pp. 154–168.
- [4] C.-M. CHEN, F. LIU, V. ANH, AND I. TURNER, *Numerical schemes with high spatial accuracy for a variable-order anomalous subdiffusion equation*, SIAM J. Sci. Comput., 32 (2010), pp. 1740–1760.

- [5] S. CHEN, F. LIU, AND K. BURRAGE, *Numerical simulation of a new two-dimensional variable-order fractional percolation equation in non-homogeneous porous media*, Comput. Math. Appl., 67 (2014), pp. 1673–1681.
- [6] S. CHEN, J. SHEN, AND L.-L. WANG, *Generalized Jacobi Functions and their Applications to Fractional Differential Equations*, preprint, arXiv:1407.8303, 2014; available online from <http://www.ams.org/journals/mcom/0000-000-00/S0025-5718-2015-03035-X/home.html>.
- [7] W. CHEN AND S. HOLM, *Fractional Laplacian time-space models for linear and nonlinear lossy media exhibiting arbitrary frequency power-law dependency*, J. Acoust. Soc. Amer., 115 (2004), pp. 1424–1430.
- [8] S. CIFANI AND E. R. JAKOBSEN, *On the spectral vanishing viscosity method for periodic fractional conservation laws*, Math. Comp., 82 (2013), pp. 1489–1514.
- [9] P. CONSTANTIN AND V. VICOL, *Nonlinear maximum principles for dissipative linear nonlocal operators and applications*, Geom. Funct. Anal., 22 (2012), pp. 1289–1321.
- [10] A. DE PABLO, F. QUIRÓS, A. RODRÍGUEZ, AND J. L. VÁZQUEZ, *A fractional porous medium equation*, Adv. Math., 226 (2011), pp. 1378–1409.
- [11] K. DIETHELM, N. J. FORD, AND A. D. FREED, *Detailed error analysis for a fractional Adams method*, Numer. Algorithms, 36 (2004), pp. 31–52.
- [12] H. DING, C. LI, AND Y. CHEN, *High-order algorithms for Riesz derivative and their applications (II)*, J. Comput. Phys., 293 (2015), pp. 218–237.
- [13] L. FATONE AND D. FUNARO, *Optimal collocation nodes for fractional derivative operators*, SIAM J. Sci. Comput., 37 (2015), pp. A1504–A1524.
- [14] B.-Y. GUO, *Spectral Methods and their Applications*, World Scientific, River Edge, NJ, 1998.
- [15] B. JIN, R. LAZAROV, Y. LIU, AND Z. ZHOU, *The Galerkin finite element method for a multi-term time-fractional diffusion equation*, J. Comput. Phys., 281 (2015), pp. 825–843.
- [16] C. LI, F. ZENG, AND F. LIU, *Spectral approximations to the fractional integral and derivative*, Fract. Calc. Appl. Anal., 15 (2012), pp. 383–406.
- [17] X. LI AND C. XU, *A space-time spectral method for the time fractional diffusion equation*, SIAM J. Numer. Anal., 47 (2009), pp. 2108–2131.
- [18] CH. LUBICH, *Discretized fractional calculus*, SIAM J. Math. Anal., 17 (1986), pp. 704–719.
- [19] H. MA AND W. SUN, *Optimal error estimates of the Legendre–Petrov–Galerkin method for the Korteweg–de Vries equation*, SIAM J. Numer. Anal., 39 (2001), pp. 1380–1394.
- [20] R. L. MAGIN, *Fractional Calculus in Bioengineering*, Begell House, Redding, CT, 2006.
- [21] F. MAINARDI, *Fractional Calculus and Waves in Linear Viscoelasticity*, Imperial College Press, London, 2010.
- [22] M. M. MEERSCHAERT AND C. TADJERAN, *Finite difference approximations for two-sided space-fractional partial differential equations*, Appl. Numer. Math., 56 (2006), pp. 80–90.
- [23] R. METZLER AND J. KLAFTER, *The random walk's guide to anomalous diffusion: A fractional dynamics approach*, Phys. Rep., 339 (2000), pp. 1–77.
- [24] K. MUSTAPHA AND W. MCLEAN, *A second-order accurate numerical method for a fractional wave equation*, Numer. Math., 3 (2007), pp. 481–510.
- [25] K. MUSTAPHA AND W. MCLEAN, *Superconvergence of a discontinuous Galerkin method for fractional diffusion and wave equations*, SIAM J. Numer. Anal., 51 (2013), pp. 491–515.
- [26] N. NIE, J. HUANG, W. WANG, AND Y. TANG, *Solving spatial-fractional partial differential diffusion equations by spectral method*, J. Stat. Comput. Simul., 84 (2014), pp. 1173–1189.
- [27] I. PODLUBNY, *Fractional Differential Equations*, Academic Press, San Diego, CA, 1999.
- [28] J. SHEN, T. TANG, AND L.-L. WANG, *Spectral Methods*, Springer Ser. Comput. Math. 41, Springer, Heidelberg, 2011.
- [29] H. SUN, W. CHEN, H. WEI, AND Y. CHEN, *A comparative study of constant-order and variable-order fractional models in characterizing memory property of systems*, Eur. Phys. J. Spec. Top., 193 (2011), pp. 185–192.
- [30] W. TIAN, H. ZHOU, AND W. DENG, *A class of second order difference approximation for solving space fractional diffusion equations*, Math. Comp., 84 (2015), pp. 1703–1727.
- [31] W. Y. TIAN, W. DENG, AND Y. WU, *Polynomial spectral collocation method for space fractional advection-diffusion equation*, Numer. Methods Partial Differential Equations, 30 (2014), pp. 514–535.
- [32] D. VALÉRIO AND J. S. DA COSTA, *Variable-order fractional derivatives and their numerical approximations*, Signal Process., 91 (2011), pp. 470–483.
- [33] H. WANG AND X. ZHANG, *A high-accuracy preserving spectral Galerkin method for the Dirichlet boundary-value problem of variable-coefficient conservative fractional diffusion equations*, J. Comput. Phys., 281 (2015), pp. 67–81.
- [34] Q. XU AND J. S. HESTHAVEN, *Stable multi-domain spectral penalty methods for fractional partial differential equations*, J. Comput. Phys., 257 (2014), pp. 241–258.

- [35] M. ZAYERNOURI, M. AINSWORTH, AND G. E. KARNIADAKIS, *A unified Petrov–Galerkin spectral method for fractional PDEs*, Comput. Methods Appl. Mech. Engrg., 283 (2015), pp. 1545–1569.
- [36] M. ZAYERNOURI AND G. E. KARNIADAKIS, *Fractional Sturm–Liouville eigen-problems: Theory and numerical approximation*, J. Comput. Phys., 252 (2013), pp. 495–517.
- [37] M. ZAYERNOURI AND G. E. KARNIADAKIS, *Exponentially accurate spectral and spectral element methods for fractional ODEs*, J. Comput. Phys., 257 (2014), pp. 460–480.
- [38] M. ZAYERNOURI AND G. E. KARNIADAKIS, *Fractional spectral collocation method*, SIAM J. Sci. Comput., 36 (2014), pp. A40–A62.
- [39] M. ZAYERNOURI AND G. E. KARNIADAKIS, *Fractional spectral collocation methods for linear and nonlinear variable order FPDEs*, J. Comput. Phys., 293 (2015), pp. 312–338.
- [40] F. ZENG AND C. LI, *Fractional Differentiation Matrices with Applications*, preprint, arXiv:1404.4429, 2014.
- [41] F. ZENG, F. LIU, C. LI, K. BURRAGE, I. TURNER, AND V. ANH, *A Crank–Nicolson ADI spectral method for a two-dimensional Riesz space fractional nonlinear reaction-diffusion equation*, SIAM J. Numer. Anal., 52 (2014), pp. 2599–2622.
- [42] H. ZHANG, F. LIU, P. ZHUANG, I. TURNER, AND V. ANH, *Numerical analysis of a new space-time variable fractional order advection-dispersion equation*, Appl. Math. Comput., 242 (2014), pp. 541–550.
- [43] Y.-N. ZHANG, Z.-Z. SUN, AND H.-L. LIAO, *Finite difference methods for the time fractional diffusion equation on non-uniform meshes*, J. Comput. Phys., 265 (2014), pp. 195–210.
- [44] Z. ZHANG, F. ZENG, AND G. E. KARNIADAKIS, *Optimal error estimates of spectral Petrov–Galerkin and collocation methods for initial value problems of fractional differential equations*, SIAM J. Numer. Anal., 53 (2015), pp. 2074–2096.
- [45] X. ZHAO, Z.-Z. SUN, AND G. KARNIADAKIS, *Second-order approximations for variable order fractional derivatives: Algorithms and applications*, J. Comput. Phys., 293 (2015), pp. 184–200.
- [46] M. ZHENG, F. LIU, I. TURNER, AND V. ANH, *A novel high order space-time spectral method for the time fractional Fokker–Planck equation*, SIAM J. Sci. Comput., 37 (2015), pp. A701–A724.
- [47] P. ZHUANG, F. LIU, V. ANH, AND I. TURNER, *Numerical methods for the variable-order fractional advection-diffusion equation with a nonlinear source term*, SIAM J. Numer. Anal., 47 (2009), pp. 1760–1781.